

NUMERICAL SOLUTION TO TASK PLANNING A ROBOT
IN TORQUE SPACE

BY

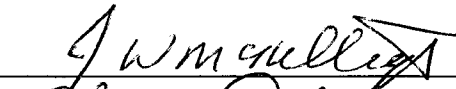
WEITIAN LIU
B.E. NATIONAL UNIVERSITY OF DEFENSE TECHNOLOGY (1996)

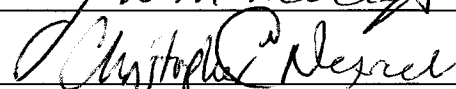
SUBMITTED IN PARTIAL FULFILLMENT OF THE REQUIREMENTS
FOR THE DEGREE OF MASTER OF SCIENCE
DEPARTMENT OF MECHANICAL ENGINEERING
UNIVERSITY OF MASSACHUSETTS LOWELL

Signature of Author: Weitian Liu Date: 5/20/2005

Signature of Thesis Supervisor: 

Robert E. Parkin, Ph.D., Professor

Signature of Other Thesis Committee Members: 



UMI Number: 1426921

INFORMATION TO USERS

The quality of this reproduction is dependent upon the quality of the copy submitted. Broken or indistinct print, colored or poor quality illustrations and photographs, print bleed-through, substandard margins, and improper alignment can adversely affect reproduction.

In the unlikely event that the author did not send a complete manuscript and there are missing pages, these will be noted. Also, if unauthorized copyright material had to be removed, a note will indicate the deletion.

UMI[®]

UMI Microform 1426921

Copyright 2005 by ProQuest Information and Learning Company.

All rights reserved. This microform edition is protected against unauthorized copying under Title 17, United States Code.

ProQuest Information and Learning Company
300 North Zeeb Road
P.O. Box 1346
Ann Arbor, MI 48106-1346

NUMERICAL SOLUTION OF TASK PLANNING A ROBOT
IN TORQUE SPACE

BY

WEITIAN LIU

ABSTRACT OF THESIS SUBMITTED TO FACULTY OF THE
DEPARTMENT OF MECHANICAL ENGINEERING
IN PARTIAL FULFILLMENT OF THE REQUIREMENTS
FOR THE DEGREE OF
MASTER OF SCIENCE
UNIVERSITY OF MASSACHUSETTS LOWELL
2005

Thesis Supervisor: Robert E. Parkin, Ph.D.
Professor, Department of Mechanical Engineering

ABSTRACT

The nonlinear dynamic systems of a one-pitch-joint link system and a two-pitch-joint link system are derived based on the joint angles. In particular, the torques required at the joints to produce the required joint motions are determined. The reverse problem of determining the joint motions based on assigned torques is fully explored. Analytical solutions are shown to be impossible, so numerical solutions are relied on.

It is shown that the motion, oscillatory and rotational, of both one and two joint systems depend on the initial conditions. For the one-pitch-joint link system, the oscillatory motion is due to gravity. For the two-pitch-joint link system, the oscillatory motion can be caused by gravity and/or the internal dynamics; the equations are so nonlinear that any attempt at linearizing is doomed to failure and approximating the system eigenvalues is not feasible.

The dynamic characteristics of the forced motion of both systems are explored, and yield some interesting responses that appear counter intuitive, but are verifiable.

ACKNOWLEDGEMENT

I would like to express my highest gratitude to my advisor, Dr. Robert E. Parkin, for his continuous advice and encouragement in pursuing this research. He helped me gain self-confidence and desire to continue my academic study. Without his support, guidance and challenges, this thesis would not have taken this final form.

Many thanks to Professor John White, in the Chemical and Nuclear Engineering Department, for his kindness help throughout this research. Thanks to all Mechanical Engineering Department faculties and staff for their support. Thanks are due to graduate students of Mechanical Engineering Department for vigorous and helpful discussions. They are Xiang Li, Lu Liu, Weiwei Li, Hui Zhang and many more.

Last but not the least, I would like to thank my mother and father for their unlimited encouragement, support and understanding.

TABLE OF CONTENTS

ABSTRACT	iii
ACKNOWLEDGEMENT	iv
TABLE OF CONTENTS	v
LIST OF FIGURE	vii
LIST OF TERMS	xii
Chapter 1 Introduction	
1.1 Introduction	1
1.2 Background	2
1.3 Thesis Objectives	3
Chapter 2 One-Pitch-Joint System	
2.1 Model of a One-Pitch-Joint System	6
2.2 Nonlinear State Space Equations	8
2.3 Characteristics in Free Motion	12
2.4 Dynamics of Forced Motion	22
2.5 Conclusion	29
Chapter 3 Two-Pitch-Joint System	
3.1 Model of a Two-Pitch-Joint System	31
3.2 Nonlinear State Space Equations	33
3.3 Characteristics in Free Motion	42
3.3.1 Characteristics in Free Motion in Case of $p = [0 \ 0 \ 1]^T$	43

3.3.2 Characteristics in Free Motion in Case of $p = [0 \ 1 \ 0]$	55
3.4 Dynamics in Forced Motion	59
3.4.1 Dynamics of Forced Motion in case of $p = [0 \ 0 \ 1]$	60
3.4.2 Dynamics of Forced Motion in case of $p = [0 \ 1 \ 0]$	60
3.5 Conclusion	66
Chapter 4 Conclusion	68
REFERENCE	70
BIOGRAPHY	72

LIST OF FIGURES

2.1	Mathematical and physical model of a one-pitch-joint link system	7
2.2	Relationships between position space, joint space and torque space	9
2.3	Angular displacement versus time for free motion at different initial conditions: $\underline{z}_0 = [0 \ 0.1]'$, $\underline{z}_0 = [0 \ 1]'$, $\underline{z}_0 = [0 \ 5]'$	13
2.4	Angular velocities versus time for free motion at different initial conditions: $\underline{z}_0 = [0 \ 0.1]'$, $\underline{z}_0 = [0 \ 1]'$, $\underline{z}_0 = [0 \ 5]'$	14
2.5	Angular accelerations versus time for free motion at different initial conditions: $\underline{z}_0 = [0 \ 0.1]'$, $\underline{z}_0 = [0 \ 1]'$, $\underline{z}_0 = [0 \ 5]'$	14
2.6	Angular displacements versus time for free motion at different initial conditions: $\underline{z}_0 = [0.1 \ 0]'$, $\underline{z}_0 = [1 \ 0]'$, $\underline{z}_0 = [5 \ 0]'$	16
2.7	Angular velocities versus time for free motion at different initial conditions: $\underline{z}_0 = [0.1 \ 0]'$, $\underline{z}_0 = [1 \ 0]'$, $\underline{z}_0 = [5 \ 0]'$.	17
2.8	Angular accelerations versus time for free motion at different initial conditions: $\underline{z}_0 = [0.1 \ 0]'$, $\underline{z}_0 = [1 \ 0]'$, $\underline{z}_0 = [5 \ 0]'$	17
2.9	Angular displacement versus time of a pendulum ($l = 1m$)	19
2.10	Periodic, separatrix and tumbling solution curves at initial condition: $\underline{z}_0 = [1 \ 1]'$, $\underline{z}_0 = [1 \ 5]'$, $\underline{z}_0 = [1 \ \sqrt{9.81}]'$ respectively	21
2.11	Angular displacement versus time at initial condition: $\underline{z}_0 = 0, \tau = 1$	23

2.12	Angular velocity versus time at initial condition: $\underline{z}_0 = \underline{0}, \tau = 1$	23
2.13	Angular acceleration versus time at initial condition: $\underline{z}_0 = \underline{0}, \tau = 1$	24
2.14	Angular displacement versus time at initial condition: $\underline{z}_0 = [\pi \ 0]', \tau = 1$	25
2.15	Angular velocity versus time at initial condition: $\underline{z}_0 = [\pi \ 0]', \tau = 1$	25
2.16	Angular acceleration versus time at initial condition: $\underline{z}_0 = [\pi \ 0]', \tau = 1$	26
2.17	Angular displacement versus time at initial condition: $\underline{z}_0 = \underline{0}, \tau = -1$	27
2.18	Angular velocity versus time at initial condition: $\underline{z}_0 = \underline{0}, \tau = -1$	27
2.19	Angular acceleration versus time at initial condition: $\underline{z}_0 = \underline{0}, \tau = -1$	28
2.20	The motion of the system and the control action	29
3.1	Model of a two-pitch-joint link system	32
3.2	1 st joint angular displacement versus time at the initial condition: $\tau_1 = 0, \tau_2 = 0, \underline{z}_0 = [0 \ 1 \ 0 \ 1]'$	45
3.3	2 nd joint angular displacement versus time at the initial condition: $\tau_1 = 0, \tau_2 = 0, \underline{z}_0 = [0 \ 1 \ 0 \ 1]'$	45
3.4	1 st joint angular velocity versus time at the initial condition: $\tau_1 = 0, \tau_2 = 0, \underline{z}_0 = [0 \ 1 \ 0 \ 1]'$	46
3.5	2 nd joint angular velocity versus time at the initial condition: $\tau_1 = 0, \tau_2 = 0, \underline{z}_0 = [0 \ 1 \ 0 \ 1]'$	47
3.6	1 st joint angular acceleration versus time at the initial condition: $\tau_1 = 0, \tau_2 = 0, \underline{z}_0 = [0 \ 1 \ 0 \ 1]'$	48

3.7	2 nd joint angular acceleration versus time at the initial condition: $\tau_1 = 0, \tau_2 = 0, \underline{z}_0 = [0 \ 1 \ 0 \ 1]'$	48
3.8	Comparison between numerical solution curve and the corresponding sine wave of 2 nd joint angular displacement	49
3.9	Comparison between numerical solution curve and the corresponding sine wave of 2 nd joint angular velocity	50
3.10	Comparison between numerical solution curve and the corresponding sine wave of 2 nd joint angular acceleration	50
3.11	1 st joint angular displacement versus time at the initial condition: $\tau_1 = 0, \tau_2 = 0, \underline{z}_0 = [0 \ 1 \ 0 \ -1]'$	51
3.12	2 nd joint angular displacement versus time at the initial condition: $\tau_1 = 0, \tau_2 = 0, \underline{z}_0 = [0 \ 1 \ 0 \ -1]'$	52
3.13	1 st joint angular velocity versus time at the initial condition: $\tau_1 = 0, \tau_2 = 0, \underline{z}_0 = [0 \ 1 \ 0 \ -1]'$	53
3.14	2 nd joint angular velocity versus time at the initial condition: $\tau_1 = 0, \tau_2 = 0, \underline{z}_0 = [0 \ 1 \ 0 \ -1]'$	53
3.15	1 st joint angular acceleration versus time at the initial condition: $\tau_1 = 0, \tau_2 = 0, \underline{z}_0 = [0 \ 1 \ 0 \ -1]'$	54
3.16	2 nd joint angular acceleration versus time at the initial condition: $\tau_1 = 0, \tau_2 = 0, \underline{z}_0 = [0 \ 1 \ 0 \ -1]'$	54
3.17	1 st joint angular displacement versus time at the initial condition: $\tau_1 = 0, \tau_2 = 0, \underline{z}_0 = [0 \ 0.5 \ 0 \ 0.5]'$	55

3.18	2 nd joint angular displacement versus time at the initial condition: $\tau_1 = 0, \tau_2 = 0, \underline{z}_0 = [0 \ 0.5 \ 0 \ 0.5]'$	56
3.19	1 st joint angular velocity versus time at the initial condition: $\tau_1 = 0, \tau_2 = 0, \underline{z}_0 = [0 \ 0.5 \ 0 \ 0.5]'$	57
3.20	2 nd joint angular velocity versus time at the initial condition: $\tau_1 = 0, \tau_2 = 0, \underline{z}_0 = [0 \ 0.5 \ 0 \ 0.5]'$	57
3.21	1 st joint angular acceleration versus time at the initial condition: $\tau_1 = 0, \tau_2 = 0, \underline{z}_0 = [0 \ 0.5 \ 0 \ 0.5]'$	58
3.22	2 nd joint angular acceleration versus time at the initial condition: $\tau_1 = 0, \tau_2 = 0, \underline{z}_0 = [0 \ 0.5 \ 0 \ 0.5]'$	59
3.23	1 st joint angular displacement versus time at the initial condition: $\tau_1 = 1, \tau_2 = 1, \underline{z}_0 = \underline{0}$	61
3.24	2 nd joint angular displacement versus time at the initial condition: $\tau_1 = 1, \tau_2 = 1, \underline{z}_0 = \underline{0}$	62
3.25	1 st joint angular velocity versus time at the initial condition: $\tau_1 = 1, \tau_2 = 1, \underline{z}_0 = \underline{0}$	62
3.26	2 nd joint angular velocity versus time at the initial condition: $\tau_1 = 1, \tau_2 = 1, \underline{z}_0 = \underline{0}$	63
3.27	1 st joint angular acceleration versus time at the initial condition: $\tau_1 = 1, \tau_2 = 1, \underline{z}_0 = \underline{0}$	63
3.28	2 nd joint angular acceleration versus time at the initial condition: $\tau_1 = 1, \tau_2 = 1, \underline{z}_0 = \underline{0}$	64

3.29

The variations of the trajectory parameter θ_2 in the case of

$m_1 = m_2 = 1kg$ and $l_1 = l_2 = 1m$ (meter), where the solid line is $\tau_{2i} = 6$, and

the dotted line is $\tau_{2i} = 5$

65

LIST OF TERMS

ODE	Ordinary Differential Equation
IVP	Initial Value Problem
BVP	Boundary Value Problem
RK4	Fourth Order Runge-Kutta Method

Chapter 1

Introduction

1.1 Introduction

Robots have been utilized in many fields such as ocean and space exploration, welfare and medical and industrial applications. Common commercial and training robots are classified into: revolute robots, cylindrical robots, Cartesian robots, polar robots, SCARA robots and unclassified robots. For the study of robotics, integration of existing technologies is crucial, including mechanical and electrical engineering, computer science and human science and engineering [5].

It is very important to know the dynamic characteristics of robot manipulators in motion control problems, but in general it is difficult to analyze the dynamics of a robot manipulator theoretically because of its nonlinear characteristics. For example, if a two-link system has a large amplitude motion, we cannot rely on linearization, and the nonlinear characteristics of the system become stronger [11,12].

The analysis of robot dynamics is very complicated. It includes two main topics. One is trajectory planning whose objective is to make the robot end effectors follow a specified trajectory and control the velocity and acceleration. If the robot has N joints, then the robot controller must make each joint ($i = 1, \dots, N$) follow specified $\theta_i(t)$, $\dot{\theta}_i(t)$, $\ddot{\theta}_i(t)$ (if joint i is revolute). This problem has closed form solution. Another

problem is torque space task planning, the mapping from torque space to joint space or position space [13]. It is difficult to design in torque space, since we have no closed form solution for determining position space or joint space from torque space. To plan a trajectory using torque space is an open, iterative procedure, since equations that describe robot dynamics are a set of coupled, second-order, nonlinear Ordinary Differential Equations (ODEs) that have no analytical solution [4,6]. For example, if we wish to minimize the execution time for a robot in moving between two position space points, the ideal method would be to determine the joint most likely to be torque-limited and drive that joint with maximum actuator acceleration, adjusting the torques at the other joints to follow the prescribed path. This is not possible in closed form. Instead, we can monitor the torques at specific points along the path and change the path or execution time so that the resulting torques are feasible; this itself is an iterative procedure. The only known method to solve this kind of problem is numerical approximation, using integration techniques such as Euler's method or Runge-Kutta methods. In the following chapters, with tools like Matlab, we will concentrate on the performance of the vertical one-pitch-joint link system and two-pitch-joint link system, and not on the underlying numerical methods and coding needed to perform the actual computations. In this thesis, commercial numerical solvers i.e. the Matlab's ODE routines, such as ode23 will be used to get numerical solution to task planning a robot in torque space under certain initial conditions [3,10].

1.2 Background

Before the time when programmable computers didn't exist, it was impossible to solve a differential equation like the equation of motion of a pendulum driven by a periodic force. That is, the solution couldn't be expressed in terms of well-known functions

like in the case of the linearized equation of motion. Nonlinear equations of motion can be solved only in rare cases analytically. For that reason, physicists tried to build their theories on linear differential equations because they are easier to solve. And indeed, the most successful theories (like electrodynamics and quantum mechanics) are based on linear differential equations. Other even older theories dealing with physical phenomenon closer to everyday experience, like fluid dynamics, were less successful because their dynamics is nonlinear. However, the advent of computers in the last decades made it possible to tackle unsolvable nonlinear problems. This possibility led to a completely different view onto dynamical systems and in association with it to a new language about dynamical systems. Nonlinear dynamics became famous because of the possibility of deterministic chaos, i.e., irregular solutions even though the equation of motion is deterministic. This behavior, that is impossible in linear dynamics, was counterintuitive and therefore attracts much attention not only by mathematicians and physicists, but also by other scientists interested in scientific topics. The subject of dynamic analysis of robot is has appeared very complicated because of the nonlinearity of the motion equations. In the thesis, we use the point-plane method of analysis which is shown to provide simpler kinematic analysis than standard formulations involving the Denavit-Hartenberg notation [4].

1.3 Thesis Objective

In this thesis, the nonlinear dynamic characteristics of both free motion and forced motion of both one-pitch-joint link system and two-pitch-joint link system are explored, and yield some interesting responses that appear counter intuitive, but are verifiable. The one-pitch-joint link system looks like an upward inverted planar

pendulum and the two-pitch-joint link system looks like a double upward inverted pendulum. Both pendulums have been fully studied for many years as an archetypal system to illustrate many of the basic features of dynamic. For example, as for the planar pendulum, when it is periodically forced, the pendulum can undergo an array of changes in state, including chaotic behavior. Its importance has equally been demonstrated by many problems of practical interest that result in mathematical models which incorporate aspects of a pendulum-like equation in one form or another; for instance, the heave excited roll response of a ship in waves. More recently the system has attracted the attention of many nonlinear researchers to explore its full nonlinear response and even the possible application of controlling chaos [19]. Although the two systems, one-pitch-joint link system and two-pitch-joint link system, described in this thesis are similar to the planar pendulum and double planar pendulum respectively, they are a little different with respect to the dynamic characteristics which will be discussed in the following chapters.

In this thesis, we will model two non-linear dynamical systems, a one-pitch-joint link system and a two-pitch-joint link system, and derive the motion equations of both systems, then simulate both of the systems numerically using ODE routine with Matlab and discuss the dynamic characteristics of both systems [8,9].

In chapter 2, we will model a one-pitch-joint link system and derive the motion equations of this system. The equations can be classified into linear and non-linear according to the orientation which is chosen. Characteristics of the free motion and dynamics of the forced motion of this system are discussed. The free motion can be classified into two types. One is rotation and the other is oscillation. Furthermore, it can be shown that the initial conditions determine which motion will appear. Some dynamic characteristics are also shown. The link of this system will keep rotating or

oscillating according to the initial conditions. In addition, an example of appropriate control sequence of the system is obtained based on the dynamics of forced motion analysis.

In chapter 3, we modeled the two-pitch-joint link system and derived the motion equations of this system. The motion equations are different when different orientations are chosen. The characteristics of the free motion mode of this system are discussed. In addition, we discussed the dynamics of the forced motion of this system for two orientations which will be specified in chapter 3. The same as chapter 2, we also give an example to obtain an appropriate control sequence of the system under one of two orientations.

Chapter 2

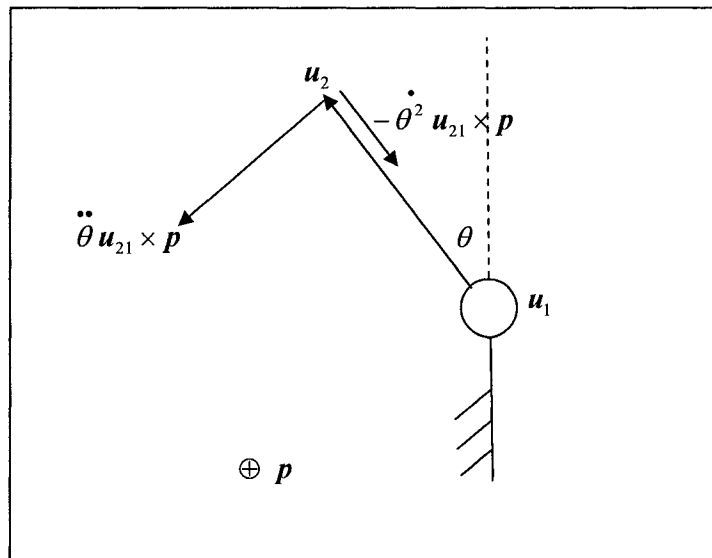
One-Pitch-Joint System

2.1 Model of a One-Pitch-Joint System

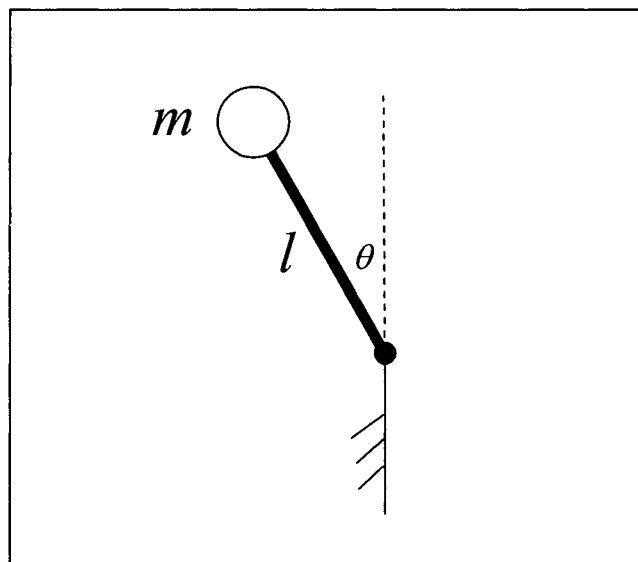
First, consider this simplest case, a vertical one-pitch-joint link system in plane p as shown in Figure 2.1. Figure 2.1 (a) is the model of one-pitch-joint link system while Figure 2.1 (b) is the corresponding physical example. In this case, we use the vector

orthogonal to the plane to define p as $p = \begin{bmatrix} a \\ b \\ c \end{bmatrix}$, and this vector is directed into the

paper. From Figure 2.1, we can see that u_{21} is the vector from the origin to the end of the link, $u_{21} \times p$ is perpendicular to u_{21} . Further, we know $u_{21} \times p \times p = -u_{21}$ since u_{21} is orthogonal to p . u_1 is the origin, u_2 is the end point of the link. θ is the angular displacement of the joint. l is the length of the link. From “Applied Robotic Analysis” (1991), the acceleration at the end of the link can be expressed as [4]:



(a)



(b)

Figure 2.1 (a) Mathematical model (b) Physical model of one-pitch-joint link system.

$$\ddot{\mathbf{u}}_2 = \ddot{\theta} \mathbf{u}_{21} \times \mathbf{p} - \dot{\theta}^2 \mathbf{u}_{21} \quad (2.1)$$

The directions of these accelerations are shown in Figure 2.1.

The acceleration of a particle due to gravity is give by $\mathbf{g} = \begin{bmatrix} 0 \\ 0 \\ 9.81 \end{bmatrix} m/\text{sec}^2$. Including

gravity, the total acceleration of the point mass m at \mathbf{u}_2 is $\ddot{\mathbf{u}}_2 = \ddot{\theta} \mathbf{u}_{21} \times \mathbf{p} - \dot{\theta}^2 \mathbf{u}_{21} - \mathbf{g}$.

Assume the rod is rigid and its mass is negligible. From Newton's second law, the force on point mass m is

$$\begin{aligned} \mathbf{f} &= m \ddot{\mathbf{u}}_2 \\ &= m(\ddot{\theta} \mathbf{u}_{21} \times \mathbf{p} - \dot{\theta}^2 \mathbf{u}_{21} - \mathbf{g}) \\ &= m(\ddot{\theta} \mathbf{u}_{21} \times \mathbf{p} - \dot{\theta}^2 \mathbf{u}_{21}) - mg \begin{bmatrix} 0 \\ 0 \\ 1 \end{bmatrix} \end{aligned} \quad (2.2)$$

So, the torque at point \mathbf{u}_1 is produced by the component of the force orthogonal to \mathbf{u}_{21} .

$$\begin{aligned} \tau &= \mathbf{f} \bullet \mathbf{u}_{21} \times \mathbf{p} \\ &= \{m(\ddot{\theta} \mathbf{u}_{21} \times \mathbf{p} - \dot{\theta}^2 \mathbf{u}_{21}) - mg \begin{bmatrix} 0 \\ 0 \\ 1 \end{bmatrix}\} \bullet \mathbf{u}_{21} \times \mathbf{p} \\ &= m \ddot{\theta} l^2 - mg \begin{bmatrix} 0 \\ 0 \\ 1 \end{bmatrix} \bullet \mathbf{u}_{21} \times \mathbf{p} \end{aligned} \quad (2.3)$$

where m, l are constants.

The geometric simplification of the gravity is based on the plane of motion \mathbf{p} , and consideration of these simplifications follows in the next equation.

2.2 Nonlinear State Space Equations

Suppose a system is driven by choosing the torques at the joints. In theory, the positions of the joints as a function of time cannot be obtained in closed form, and

instead an approximate solution must be obtained involving numerical integration – the replacement of the differential equations by difference equations via the application of a numerical integration formula. This contrasts to the reverse problem, i.e. given the joints positions as a function of time we can obtain the torques necessary to drive the joints in closed form [7, 14]. The problem is shown in Figure 2.2.

The torques in a system of n revolute joints $\Theta_i, i = 1, 2, \dots, n$ is described by n second order differential equations. These are transformed to a set of $2n$ first order equations under the substitutions $z_1 = \Theta_1, z_2 = \dot{\Theta}_1, z_3 = \Theta_2, z_4 = \dot{\Theta}_2, \dots, z_{2n-1} = \Theta_n, z_{2n} = \dot{\Theta}_n$.

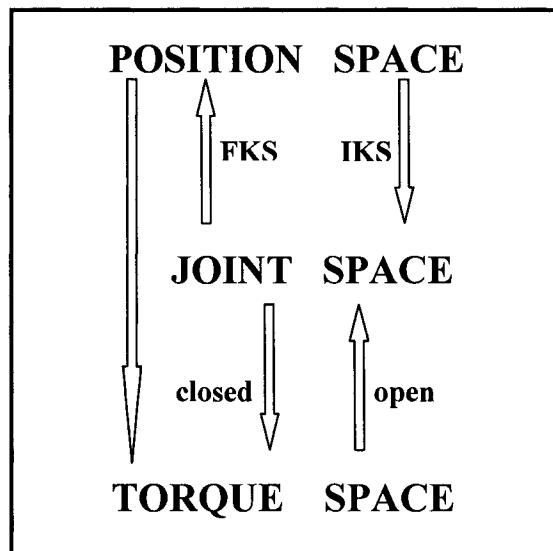


Figure 2.2 Relationships between position space, joint space and torque space.

When an orientation is chosen for the chain of links and joints, there may be some simplifications made to the terms involving gravity. In Figure 2.2, FKS, IKS denote Forward Kinematic Solutions and Inverse Kinematic Solutions respectively; closed and open denote closed form solutions and open form solutions respectively.

As for the one-pitch-joint link system, for example, suppose $\mathbf{p} = \begin{bmatrix} 0 \\ 0 \\ 1 \end{bmatrix}$ in equation (2.3),

then since $\mathbf{g} \bullet \mathbf{u}_{21} \times \mathbf{p} = 0$, the gravity term becomes zero and equation (2.3) becomes

$$\tau = m\ddot{\theta}l^2 \quad (2.4)$$

Next, suppose $\mathbf{p} = \begin{bmatrix} 0 \\ 1 \\ 0 \end{bmatrix}$, equation (2.3) becomes

$$\begin{aligned} \tau &= m\ddot{\theta}l^2 - mg \begin{bmatrix} 0 \\ 0 \\ 1 \end{bmatrix} \bullet \mathbf{u}_{21} \times \mathbf{p} \\ &= m\ddot{\theta}l^2 - m \begin{bmatrix} 0 \\ 0 \\ g \end{bmatrix} \bullet \begin{bmatrix} l \sin \theta \\ 0 \\ l \cos \theta \end{bmatrix} \times \begin{bmatrix} 0 \\ 1 \\ 0 \end{bmatrix} \\ &= m\ddot{\theta}l^2 - mgl \sin \theta \end{aligned} \quad (2.5)$$

So, this system is linear when $\mathbf{p} = \begin{bmatrix} 0 \\ 0 \\ 1 \end{bmatrix}$; and it is a nonlinear when $\mathbf{p} = \begin{bmatrix} 0 \\ 1 \\ 0 \end{bmatrix}$. The

objective here is to find the dynamic characteristics of this system. That is, the relationships of joint angular displacement (θ) versus time, joint angular velocity ($\dot{\theta}$) versus time and joint angular acceleration ($\ddot{\theta}$) versus time, when the torque (τ) is given. As for equation (2.4), that means we should try to find the analytical solution of this linear second-order differential equation. Obviously, it is very easy to find the analytical solution $\ddot{\theta} = \frac{\tau(t)}{ml^2}$, and there is no natural response;

$\dot{\theta} = \frac{1}{ml^2} (\int \tau(t) dt + a)$ and $\theta = \frac{1}{ml^2} (\iint \tau(t) dt dt + at + b)$ where a and b are determined

by the initial conditions. As for equation (2.5), through observation we find that it is

nonlinear in θ due to the term $\sin \theta$ and cannot be solved in terms of elementary functions. That is, it is impractical to find the analytical solution of this equation. In general, when an analytical solution is not possible for a nonlinear system, a numerical approximation to the solution of the nonlinear differential equation might be found by using appropriate simulation methods. We will focus on the numerical

solution to the system in the case of $p = \begin{bmatrix} 0 \\ 1 \\ 0 \end{bmatrix}$ and its dynamic characteristics in this

chapter.

Numerical solution techniques for ordinary differential equations are divided into methods that solve initial value problems (IVP), as applied here or methods that solve boundary value problems (BVP). The techniques applicable to initial value problems (IVP) are designed to solve the following n-dimensional nonlinear first order system of ordinary differential equations over the specified time interval $\alpha \leq t \leq \beta$.

$$\frac{d}{dt} \underline{z} = \underline{f}(\underline{z}, u, t) \quad (2.6)$$

Equation (2.6) is called standard state form [1]. So if we want to get the numerical solution of this ordinary differential equation group, we need put it into standard state form. To put this equation into standard state form, we make the following substitution:

$$z_1 = \theta \quad z_2 = \dot{\theta} = \dot{z}_1 \quad (2.7)$$

Write the final state space equations for the one-pitch joint $|\theta|$ as:

$$\dot{\underline{z}} = \begin{bmatrix} \dot{z}_1 \\ \dot{z}_2 \end{bmatrix} = \begin{bmatrix} \dot{\theta} \\ \ddot{\theta} \end{bmatrix} = \begin{bmatrix} z_2 \\ \frac{\tau}{ml^2} + \frac{g}{l} \sin z_1 \end{bmatrix} \quad (2.8)$$

This expression is now the desired form given in equation (2.6).

So far, we can simulate this system in Matlab using its ode23 routine. This routine applies an adaptive step control algorithm by obtaining error estimates using two Runge-Kutta (RK) predictions of different order [1]. This routine is quite accurate for many complicated cases like this one. We will discuss the dynamic characteristics of this system in following sections. Although the approximation is quite accurate, it is not true solution. There is a need to verify the approximate results, and this can be done by measuring the energy in the system. It will be noted in the following sections.

2.3 Characteristics in Free Motion

The free motion of this system can be classified into two types: rotation and oscillation. Furthermore, we can also show that the initial condition, that is, initial joint angular displacement and initial joint angular velocity, determines which motion mode will appear. In this section, four cases will be discussed in the model of free

motion of one-pitch-joint link system in case of $\underline{p} = \begin{bmatrix} 0 \\ 1 \\ 0 \end{bmatrix}$. In addition, assume point

masses $m_1 = 1kg$, link lengths $l_1 = 1m$.

Case 1: The initial kinetic energy of the system and initial joint angular displacement

are zeros in the free motion. Under this condition, $\underline{z}_0 = \underline{0} = \begin{bmatrix} 0 \\ 0 \end{bmatrix}$, the one-pitch-joint

link system will remain at rest. It is an ideal status which can not exist in practice.

Case 2: The initial kinetic energy of this system is a constant (not zero) and the initial joint angular displacement is zero.

In this case, let the initial angular velocity $\dot{\theta} = 0.1, 1, 5$ radian/sec while initial joint angular displacement $\theta = 0$, respectively and simulate this system. Figure 2.3 through

Figure 2.5 are the plots that represent the relationships of joint angular displacement versus time, joint angular velocity versus time and joint angular acceleration versus time of one-pitch-joint link for some variations of initial conditions respectively.

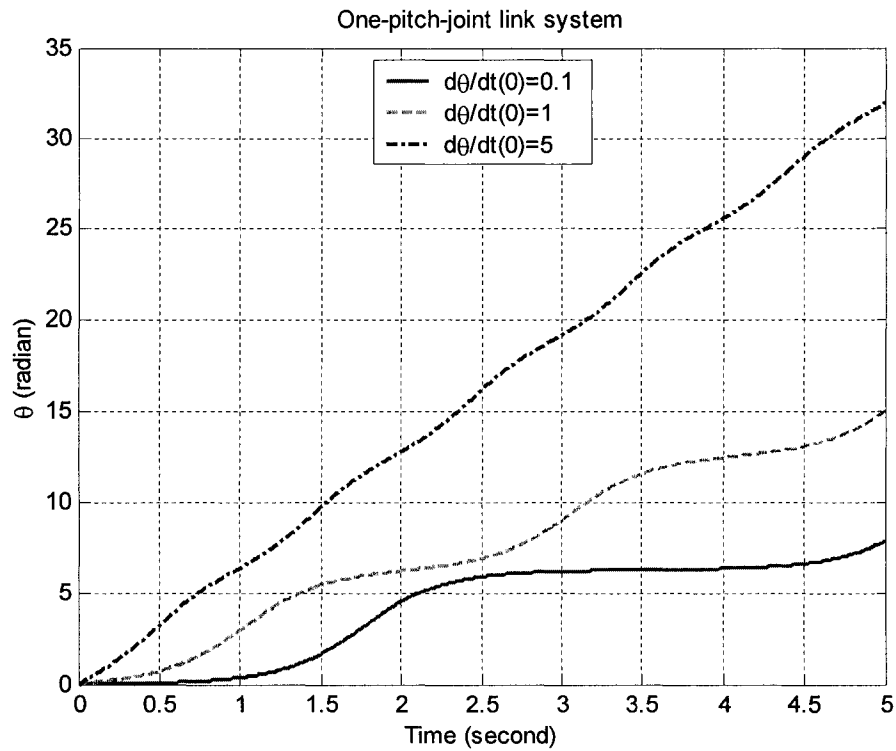


Figure 2.3 Angular displacement versus time for free motion at different initial conditions: $\underline{z}_0 = [0 \ 0.1]'$, $\underline{z}_0 = [0 \ 1]'$, $\underline{z}_0 = [0 \ 5]'$.

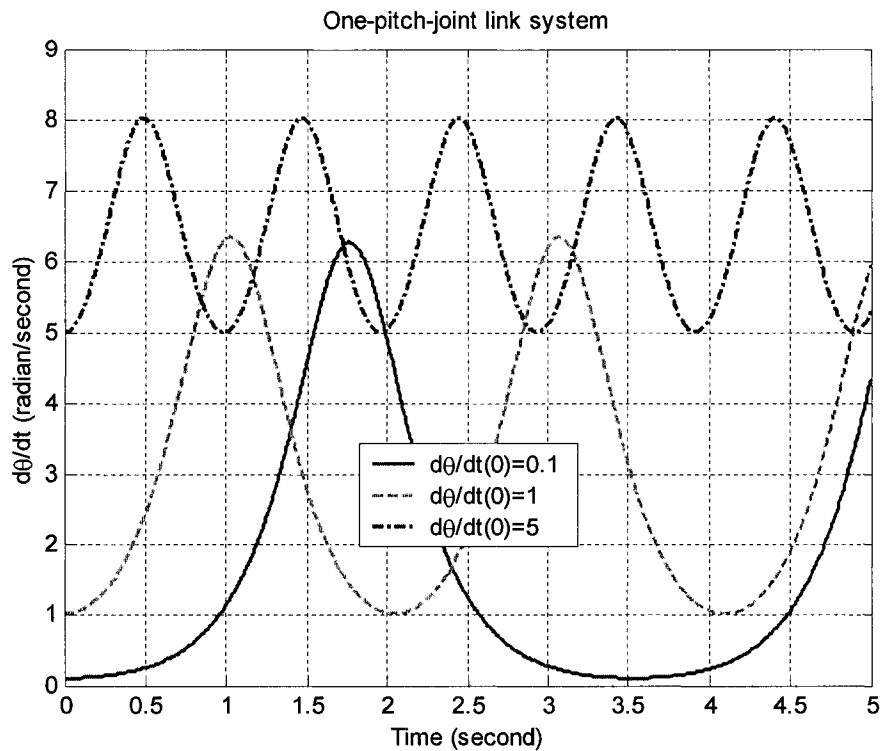


Figure 2.4 Angular velocities versus time for free motion at different initial conditions: $\underline{z}_0 = [0 \ 0.1]'$, $\underline{z}_0 = [0 \ 1]'$, $\underline{z}_0 = [0 \ 5]'$.

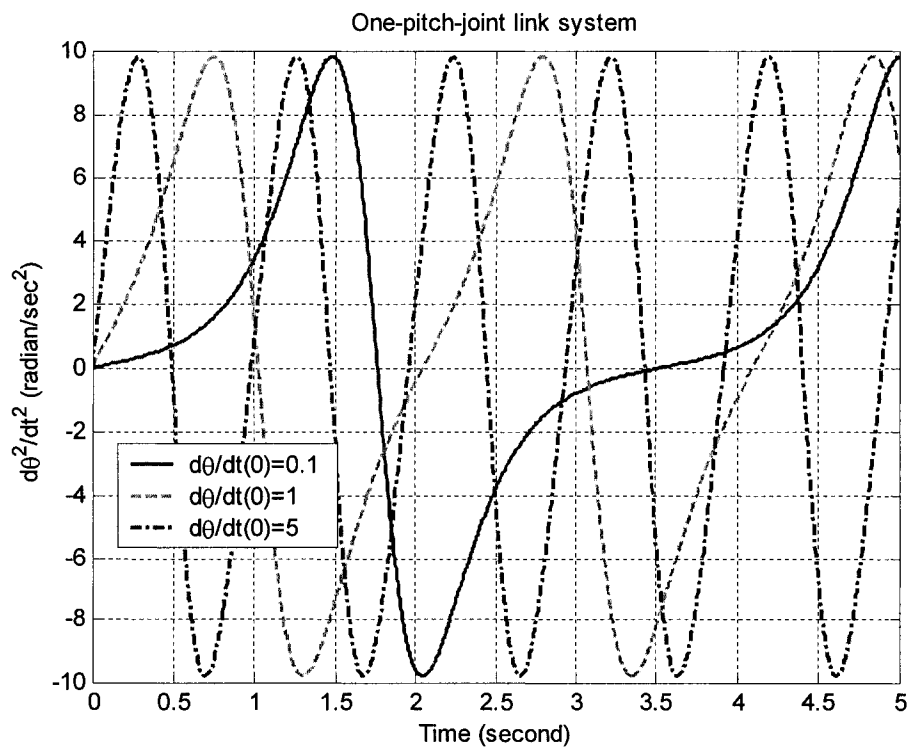


Figure 2.5 Angular accelerations versus time for free motion at different initial conditions: $\underline{z}_0 = [0 \ 0.1]'$, $\underline{z}_0 = [0 \ 1]'$, $\underline{z}_0 = [0 \ 5]'$.

From Figure 2.3, we can see that the curves look like wavy lines and they tend to be straight lines while the initial joint angular velocity increases. Also, joint angular displacement increases continuously along with the time. The greater the initial joint angular velocity is, the bigger the value of the joint angular displacement that the link rotates is within a fixed time interval. So the solution curves in Figure 2.3 are what we expect. From Figure 2.4, the solution curves look like sine waves and have different periods according to different initial joint angular velocities. It is very easy to understand this phenomenon according to the conservation of energy law. In this case, we can treat this one-pitch-joint link system as an undamped, undriven system [15,18]. So the mechanical energy (the sum of the kinetic energy and the potential energy) of this system keeps unchanged. That means the kinetic energy and potential energy of this system will convert periodically while the mechanical energy keeps unchanged. When the link rotates $(2n + 1)\pi$, $n = 0,1,2,\dots$, that is, the point mass rotates from top to the bottom, all of the potential energy of this system has converted to kinetic energy. So the kinetic energy becomes the maximum value. That is, the velocity becomes the maximum value. For example, as for the top solution curve ($\frac{d\theta}{dt}(0) = 5$) in Figure 2.4, we can see that when the angular velocity of the link become the maximum value, the corresponding joint angular displacement in Figure 2.3 is $(2n + 1)\pi$, $n = 0,1,2,\dots$ respectively. It verifies that the simulation is correct. We can also get the periods of the curves shown on the plots through analytical solution. Many studies on the analytical solutions have been carried on. It will not be repeated here. As for the joint angular acceleration, it is calculated from the formula $\ddot{\theta} = g \sin \theta$ (since $\tau = 0$). The plot can be seen in Figure 2.5.

Therefore, we can conclude: when the initial joint angular displacement is zero while initial angular velocity is a constant (not zero), the link of the system will rotate continuously.

Case 3: The initial kinetic energy is zero and the initial joint angular displacement is a constant (not zero).

In this case, let the initial joint angular displacement $\theta = 0.1, 1, 5$ while initial angular velocity $\dot{\theta} = 0$ and simulate this system. Figure 2.6 through Figure 2.8 are the plots that represent the relationships of joint angular displacement versus time, joint angular velocity versus time and joint angular acceleration versus time of one-pitch-joint link for some variations of initial conditions respectively.

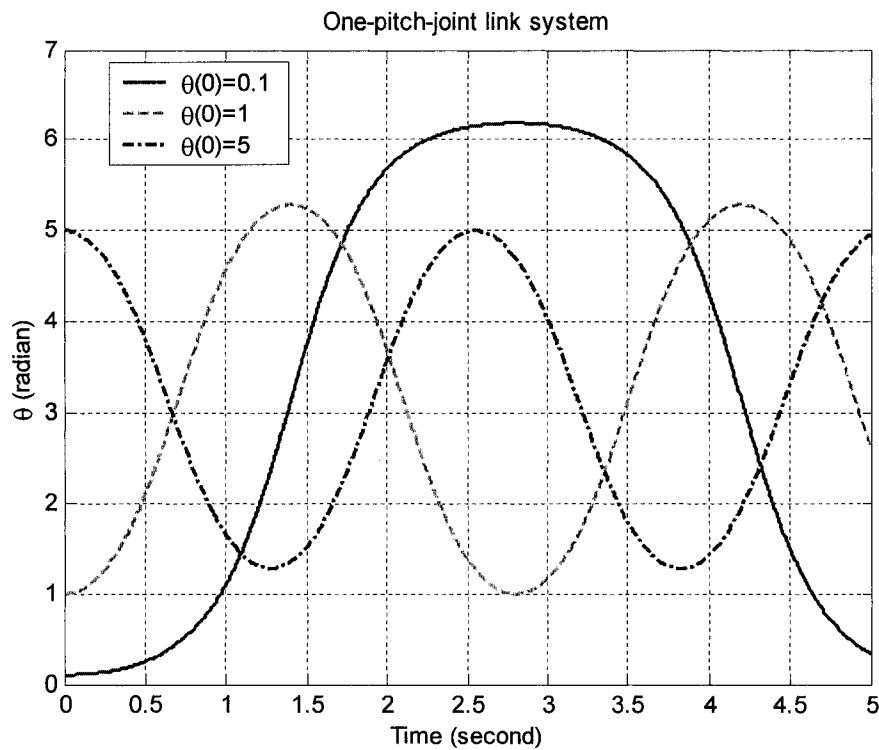


Figure 2.6 Angular displacements versus time for free motion at different initial conditions: $\underline{z}_0 = [0.1 \ 0]'$, $\underline{z}_0 = [1 \ 0]'$, $\underline{z}_0 = [5 \ 0]'$.

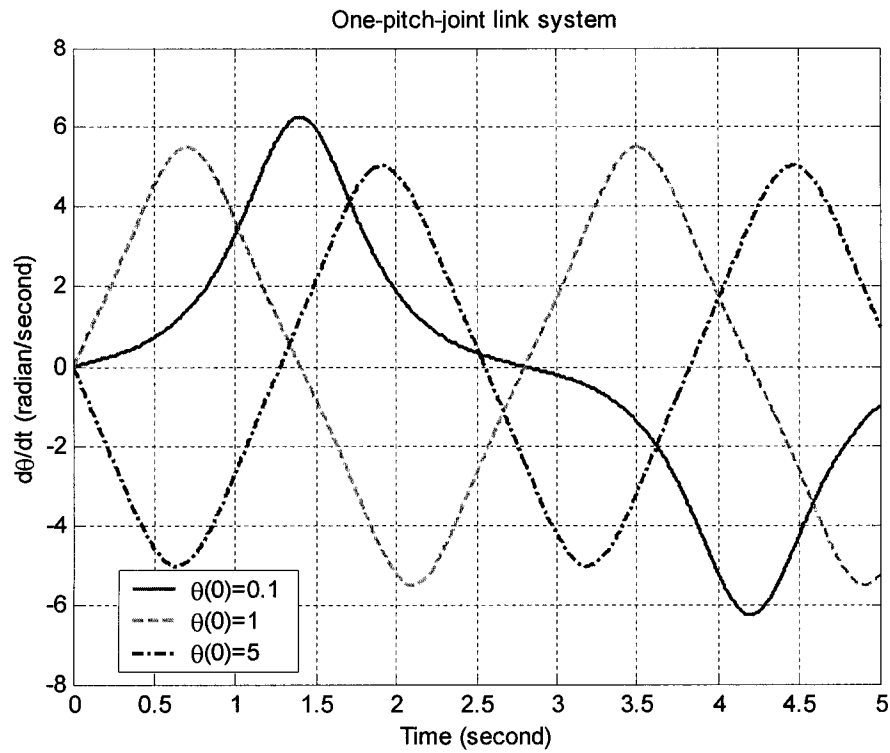


Figure 2.7 Angular velocities versus time for free motion at different initial conditions: $\underline{z}_0 = [0.1 \ 0]'$, $\underline{z}_0 = [1 \ 0]'$, $\underline{z}_0 = [5 \ 0]'$.

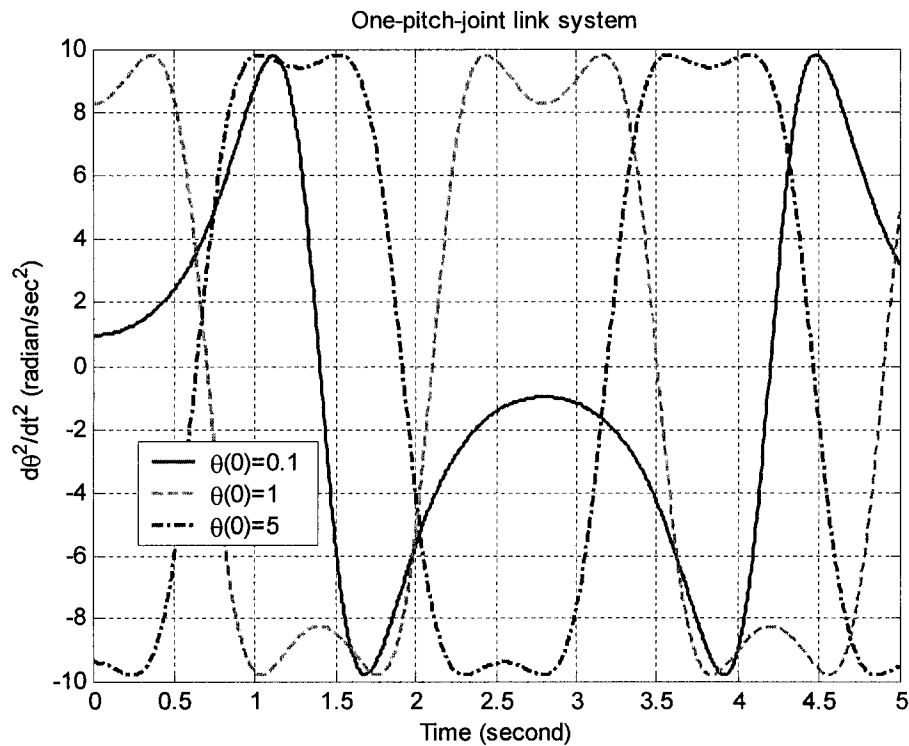


Figure 2.8 Angular accelerations versus time for free motion at different initial conditions: $\underline{z}_0 = [0.1 \ 0]'$, $\underline{z}_0 = [1 \ 0]'$, $\underline{z}_0 = [5 \ 0]'$.

From Figure 2.6, we can see that the solution curves are sine wave alike and have different period according to different initial joint angular displacement. It means that the link of one-pitch-joint system will oscillate between two points. In addition, we can also explain this phenomenon according to the conservation of energy law. It will not be discussed in detail here since it is similar to case 2. As for the angular velocity and angular acceleration, it is indicated in Figure 2.7 and Figure 2.8.

So we can conclude: when the initial angular velocity is zero while the initial joint angular displacement is a constant (not zero), the link of this system will oscillate between two specified points which can be specified.

One thing should be noted here. When the initial angular displacement is nearby π , that is, $\theta(0)$ is within $180^\circ \pm 5^\circ$, this one-pitch-joint link can be seen as a harmonic

oscillator. We can calculate its period of oscillation through $T = 2\pi\sqrt{\frac{l}{g}}$ where l is the

length of the link. It indicates that the period of the harmonic oscillator is only dependent on the length of the link. Figure 2.9 is the example of the plot which represents the relationship of the angular displacement versus time of a harmonic oscillator with the length of the link is $l=1\text{ m}$. It can be seen from Figure 2.9 that the period is about 2 seconds although the initial angular displacements are different.

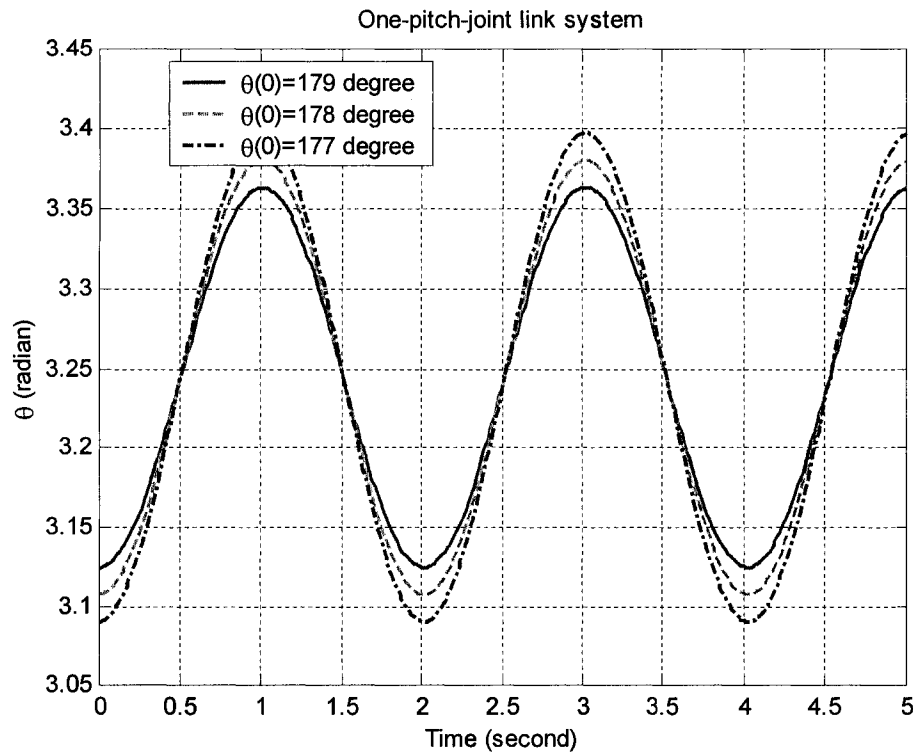


Figure 2.9 Angular displacement versus time of a pendulum ($l = 1m$).

This one-pitch-joint link system is properly modeled by a harmonic oscillator only for small angular displacement range, that is, $\theta(0)$ is within $180^\circ \pm 5^\circ$. It is well known from the experiment done by researchers that the period of oscillation increases with increasing amplitude of oscillation. Starting near the upside-down position, you will find that the period becomes much larger than for small-angle oscillations. In fact, the period approaches infinity in the limit $\theta_{\max} \rightarrow 0^\circ$. In the virtual lab (and in reality too) you will never reach this limit. This system can be treated as an undamped and undriven pendulum. Although the motion equation is *nonlinear*, we can calculate its period as a function of the amplitude θ_{\max} . The formula is given as:

$$T = \frac{4}{\omega_0} K\left(\frac{\theta_{\max}}{2}\right),$$

$$K(0) = \frac{\pi}{2}, K(\theta \rightarrow \frac{\pi}{2}) \rightarrow \infty, K(\theta) = \frac{\pi}{2} \left(1 + \frac{\theta^2}{4} + \dots\right), \omega_0 = \sqrt{\frac{g}{l}}.$$

Where g is the gravity constant, l is the length of the link. Use this formula, we can verify the periods of the solution curves. For example, we calculated the periods of the solution curves of Figure 2.6 are 5.8s, 2.74s, 2.55s which coincide with the plots. Therefore, the simulation results are verified.

Case 4: The initial kinetic energy and the initial joint angular displacement are constants (but not zeros).

In this case, the link of this system may rotate continuously (tumbling curves for joint angle displacement) or oscillate (periodic curves for joint angle displacement) between two specified points according to the values of initial kinetic energy and initial joint angular displacement. The curves that are hardest to find are those that separate the periodic curves from the tumbling curves. This kind of curve is called *separatrix*. Figure 2.10 shows the solution curves of the one-pitch-joint link system at the initial conditions: $\underline{z}_0 = [1 \ 1]$ (periodic back-and-forth motion), $\underline{z}_0 = [1 \ 5]$ (tumbling motion over the pivot) and $\underline{z}_0 = [1 \ \sqrt{9.81}]$ (*separatrix* motion) [2]. The number $\sqrt{9.81}$ is exact but computer arithmetic is not, so we had to start a little below $\sqrt{9.81}$ to even come close to the separatrix solution shown.

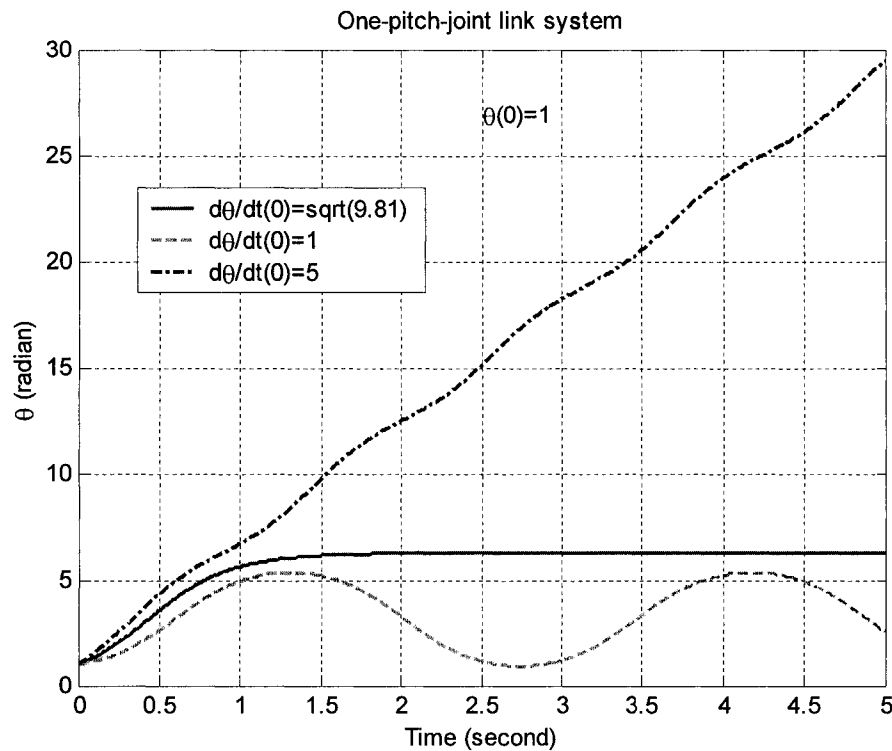


Figure 2.10 Periodic, separatrix and tumbling solution curves at initial condition:

$$\underline{z}_0 = [1 \quad 1], \underline{z}_0 = [1 \quad 5], \underline{z}_0 = [1 \quad \sqrt{9.81}] \text{ respectively.}$$

It is easy to explain these three solution curves according to the conservation of energy law. From Figure 2.10, the initial joint angular displacement is fixed as 1 radian from the vertical direction. When the initial joint angular velocity equals to 1 radian/second, the link will oscillate between two specified points because the link has not enough kinetic energy to overcome the gravity of the point mass to rotate continuously. The critical joint angular velocity is $\sqrt{9.81}$. When the initial joint angular velocity is greater than the critical velocity, for example, 5, the link tumbles over the joint because it has enough kinetic energy to overcome the gravity to rotate continuously.

Up to now, the discussion of solution curves is based on an examination of the plots in Figure 2.3 through Figure 2.10 which are generated by a numerical solver.

Fortunately, these properties can be explained according the conservation of energy law and the simulation results can be verified through empirical formula.

2.4 Dynamics of Forced Motion

In this section, we will discuss the dynamics of forced motion and can easily obtain an appropriate control sequence so as to move the system along the specified path. We simulated this system under different initial conditions and find that the link of this system keeps rotating or oscillating according to the initial conditions when the actuated torque is constant at the joint. We will consider two cases.

Case 1: the link of this system keeps rotating.

Assume point mass $m_1 = 1kg$, link length $l = 1m$ and simulate this system under the

initial condition: $\underline{z}_0 = \underline{0} = \begin{bmatrix} 0 \\ 0 \end{bmatrix}$, $\tau = 1$. Figure 2.11 through Figure 2.13 the plots that

represent relationships of joint angular displacement versus time, angular velocity versus time and angular acceleration versus time under this initial condition.

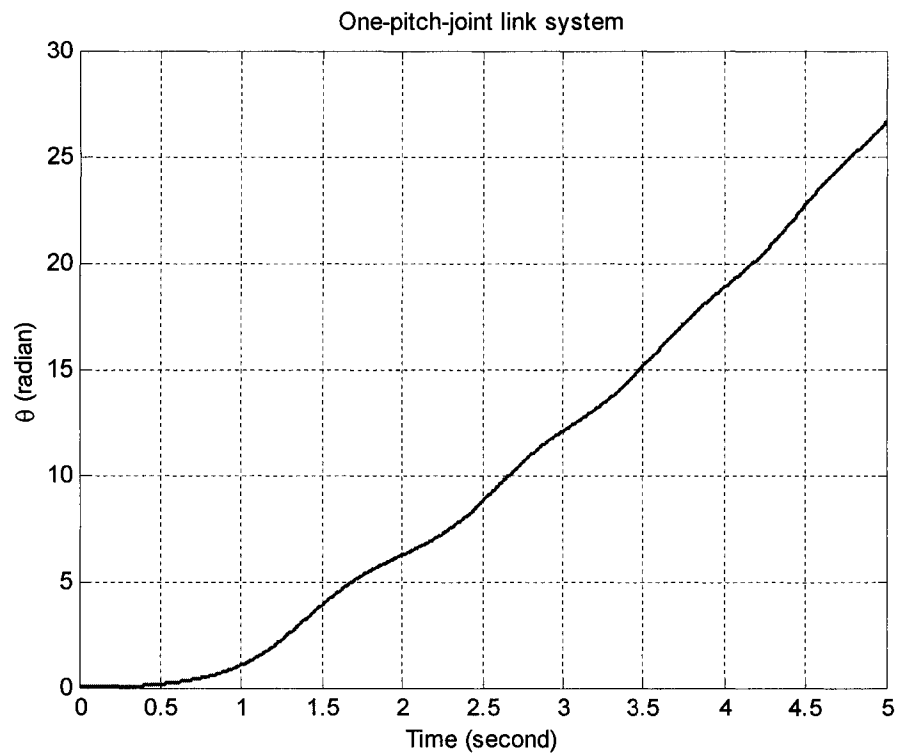


Figure 2.11 Angular displacement versus time at initial condition: $\underline{z}_0 = \underline{0}, \tau = 1$

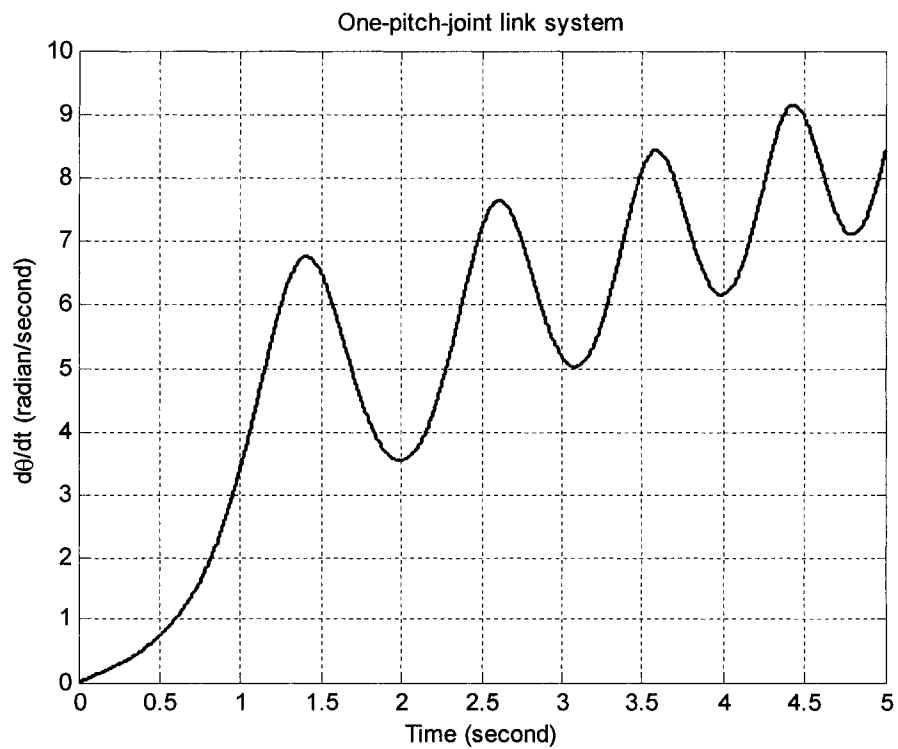


Figure 2.12 Angular velocity versus time at initial condition: $\underline{z}_0 = \underline{0}, \tau = 1$

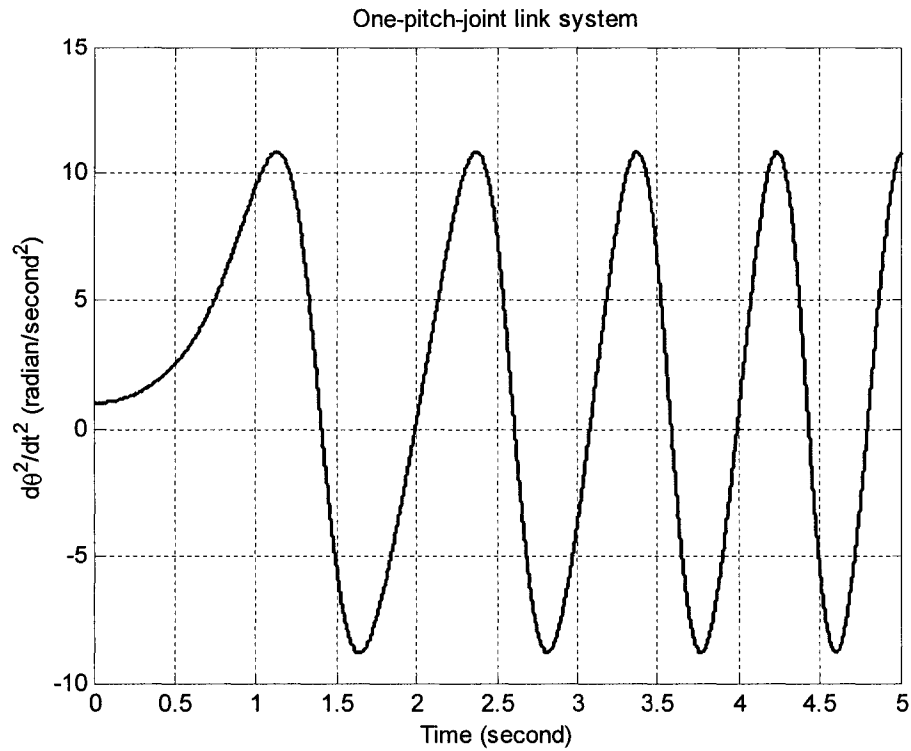


Figure 2.13 Angular acceleration versus time at initial condition: $\underline{z}_0 = \underline{0}, \tau = 1$

From Figure 2.11, we can see that the link of this system keeps rotating. From Figure 2.12 and Figure 2.13, we can see that the angular velocity of the system keeps increasing and the angular acceleration oscillates within the specified amplitude when the actuated torque is constant over the time interval. It is very easy to understand according the physical characteristics of this system and will not be explained in detail.

Case 2: the link of this system keeps oscillating.

Assume point mass $m_1 = 1kg$, link length $l = 1m$ again and simulate this system under the initial condition: $\underline{z}_0 = [\pi \ 0]^T, \tau = 1$. Figure 2.14 through Figure 2.16 are the plots that represent relationships of joint angular displacement versus time, angular velocity versus time and angular acceleration versus time under this initial condition.

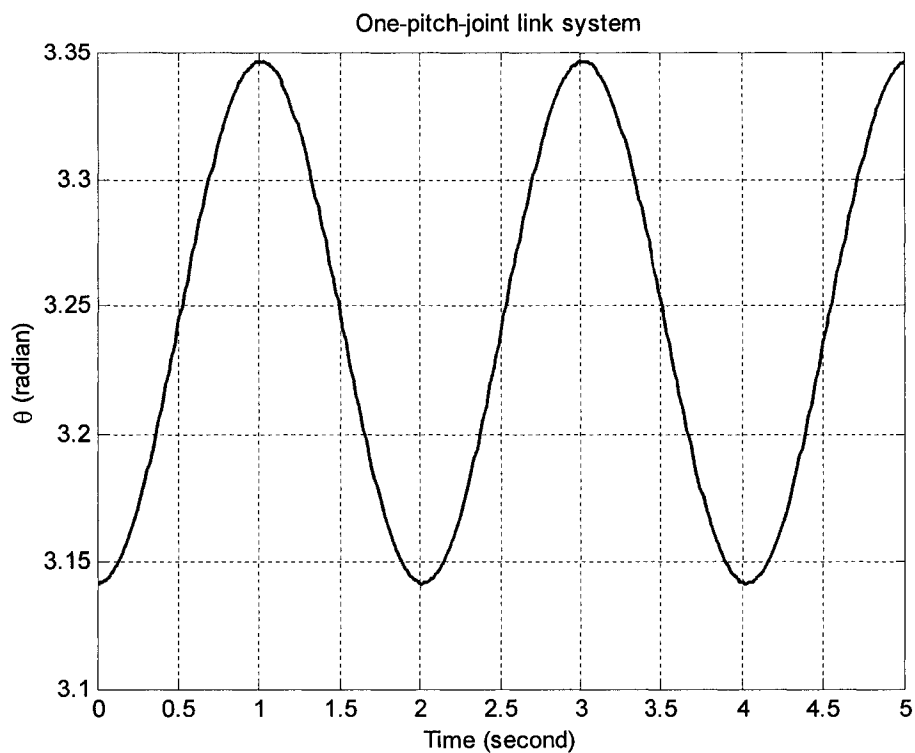


Figure 2.14 Angular displacement versus time at initial condition: $\underline{z}_0 = [\pi \ 0]$, $\tau = 1$

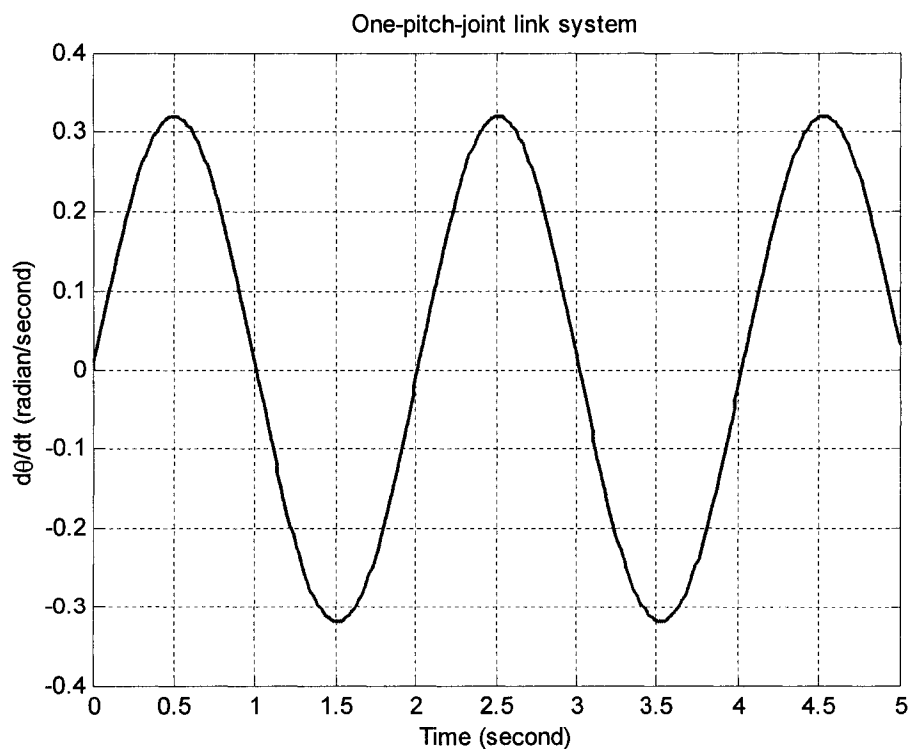


Figure 2.15 Angular velocity versus time at initial condition: $\underline{z}_0 = [\pi \ 0]$, $\tau = 1$

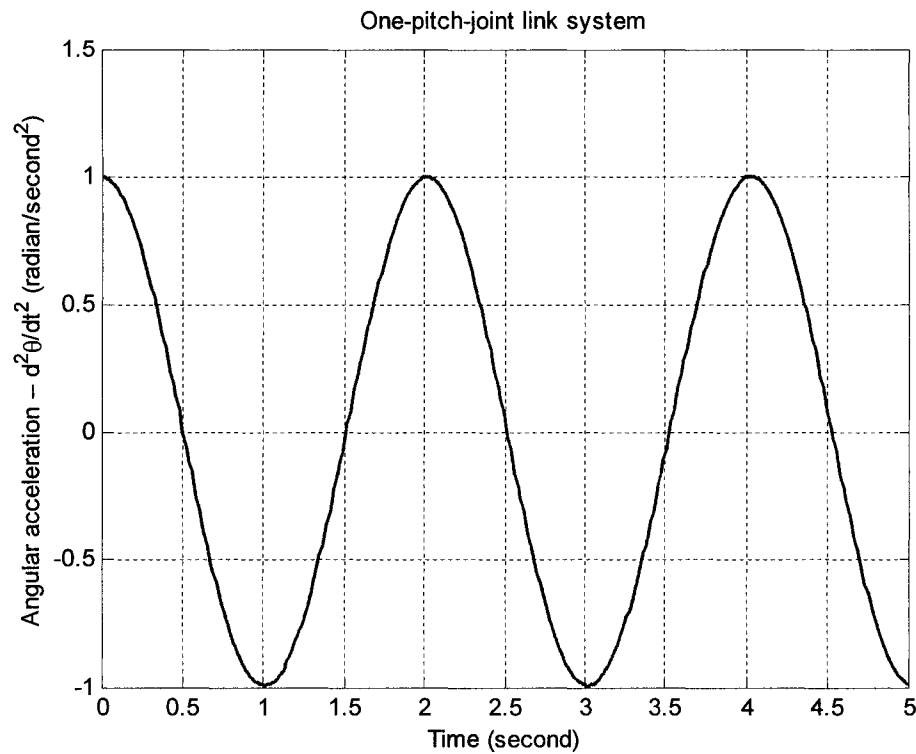


Figure 2.16 Angular acceleration versus time at initial condition: $\underline{z}_0 = [\pi \ 0]$, $\tau = 1$

From Figure 2.14, we can see that the link of this system keeps oscillating between two specified points. It is easy to understand. The actuated torque is not big enough to overcome the gravity force to keep the link tumbling over the pivot. So the link of this system keeps oscillating.

To obtain an appropriate control sequence, we keep the initial condition in case 1 unchanged and let the actuated torque equal to -1. Simulate this system and see what will happen. Figure 2.17 through Figure 2.19 are the plots that represent relationships of joint angular displacement versus time, angular velocity versus time and angular acceleration versus time under the initial condition: $\underline{z}_0 = \underline{0}$, $\tau = -1$.

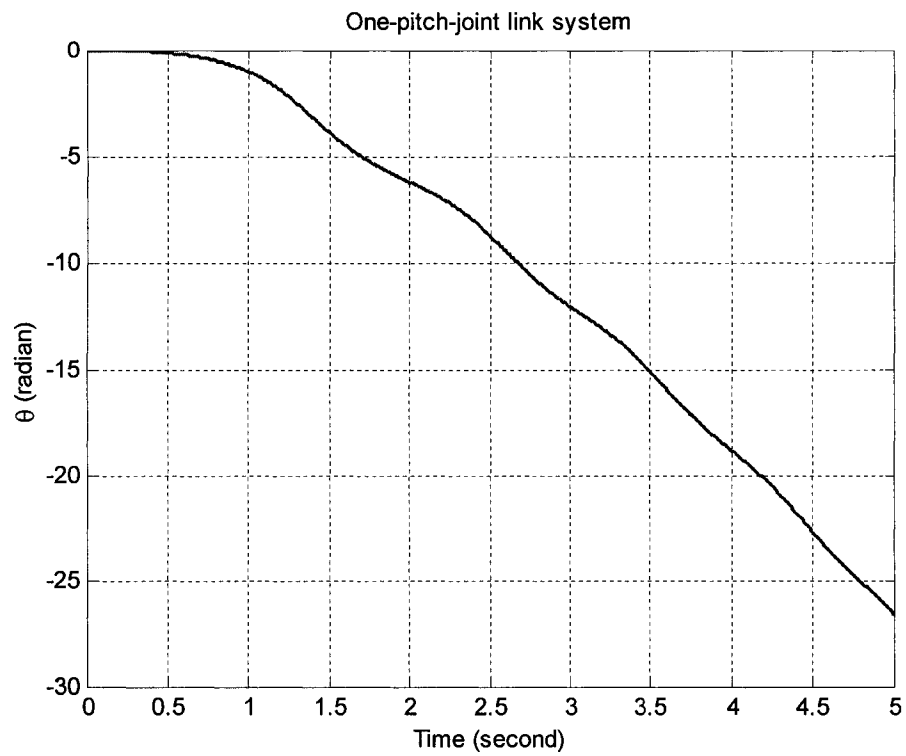


Figure 2.17 Angular displacement versus time at initial condition: $\underline{z}_0 = \underline{0}, \tau = -1$

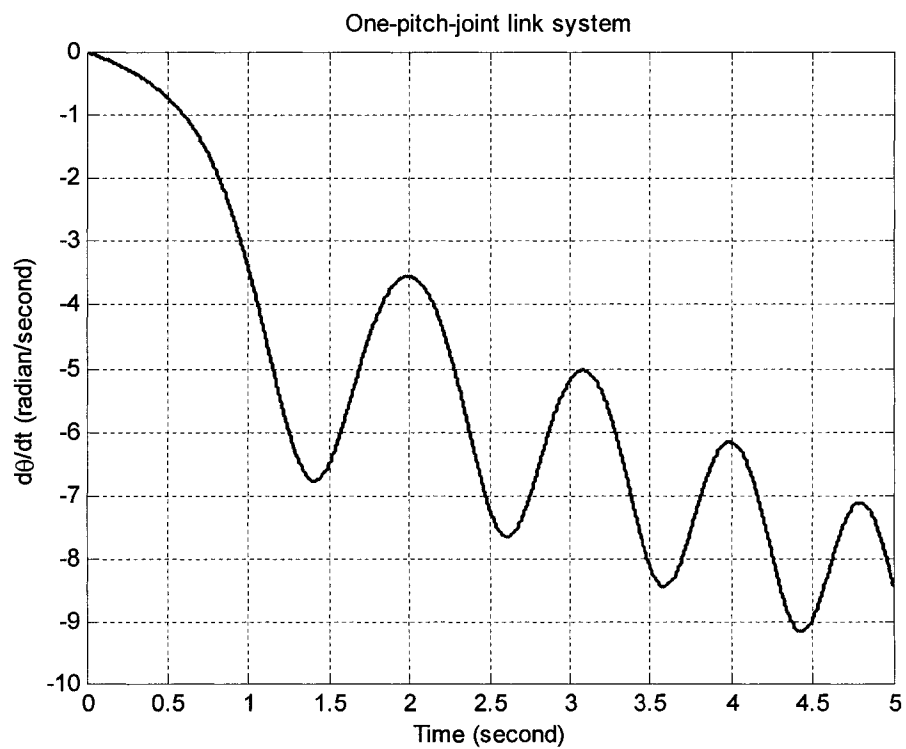


Figure 2.18 Angular velocity versus time at initial condition: $\underline{z}_0 = \underline{0}, \tau = -1$

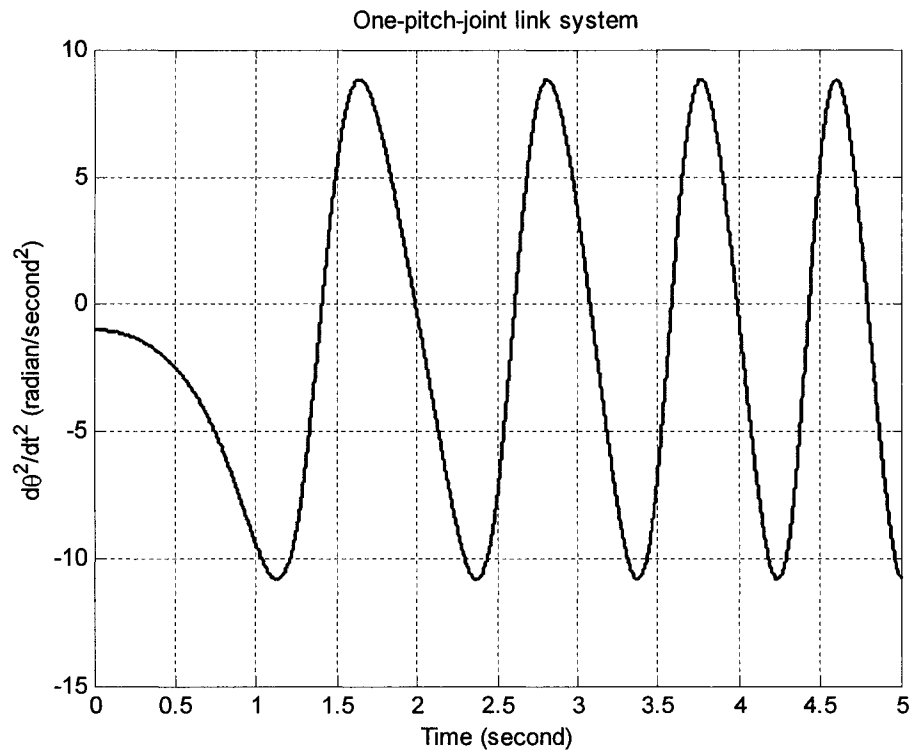


Figure 2.19 Angular acceleration versus time at initial condition: $\underline{z}_0 = \underline{0}, \tau = -1$

It can be seen that Figure 2.17 through Figure 2.19 are the inverse cases of Figure 2.11 through Figure 2.13 respectively. So we can assume that the motion of this system can be controlled along a specified path. The example of control action and the motion of the system as a function of time are shown in Figure 2.20. From Figure 2.20, we can see that the negative torque must be continued slightly longer to move the point mass (the endpoint of the link) to the specified point with zero velocity at this endpoint. It shows that the objective of control was successfully achieved.

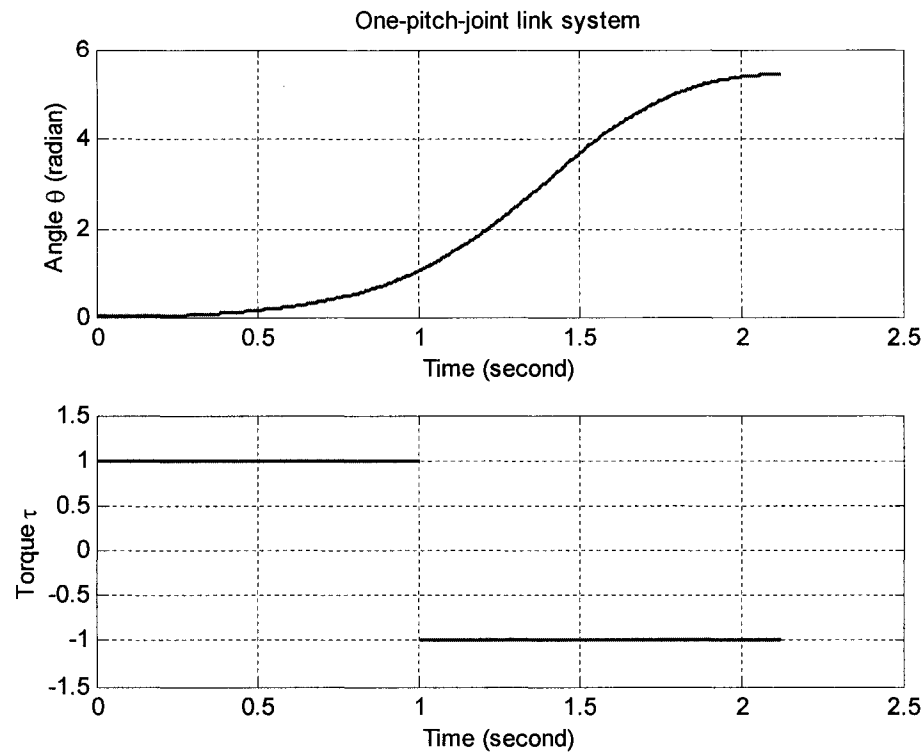


Figure 2.20 The motion of the system and the control action.

Figure 2.20 is only a simple example of control action. However, from this example, we can predict: as long as the actuated torque and switched point are given, we can take the motion trajectory schematically by the similar manner in this example. Again, we recognize the importance of the dynamics characteristics of a system, including that of free motion and forced motion. It is the fundamental of the motion control action.

2.5 Conclusion

In this chapter, we modeled a one-pitch-joint link system and drove the motion equation of this system. The equations can be classified into linear and non-linear according to the orientation which is chosen. Characteristics of the free motion and dynamics of the forced motion of this system are discussed. The free motion can be classified into two types. One is rotation and the other is oscillation. Furthermore, is

can be shown that the initial conditions determine which motion will appear. Some dynamic characteristics are also shown. The link of this system will keep rotating or oscillating according to the initial conditions. In addition, an example of appropriate control sequence of the system is obtained based on the dynamics of forced motion analysis. Meanwhile, we know that as long as the actuated torque and switched points are given, we can take the motion trajectory schematically by the manner in the control example.

Chapter 3

Two-Pitch-Joint System

3.1 Model of a Two-Pitch-Joint System

As mentioned in chapter 1, it is generally difficult to analyze the dynamics of a robot manipulator analytically because of its non-linear characteristics. For example, if a two-pitch-joint link system has a large amplitude motion, we can not rely on linearization, and the non-linear characteristics of the system become stronger. For this reason, it seems that there are few studies on the theoretical analysis of dynamics of a two-pitch-joint link system. However, it is known that first integrals of non-linear differential equations give qualitative information about the behavior of the underlying dynamical systems, and there are some studies on finding the first integrals of non-linear dynamical systems and their application. For example, Kowalski and Steeb discussed the problem of finding symmetries and first integrals for non-linear dynamical systems using the Hilbert space approach [17]. Sarlet and others discussed the approach for finding the first integrals of some non-linear dynamical equations. Moreover, the motion analysis of a cart pendulum using first integral has been studied.

Kee-Ho Yu, Takayuki Takahashi and Hikaru Inooka presented the non-linear motion analysis of a horizontal two-pitch-joint link system by focusing on the constant of the

first integrals. In their paper, they derived the equations of motion and showed that the first integrals can be obtained for the system. The procedure of the derivation is described as following:

The two-pitch-joint system which has planar motion without friction and damping effect is modeled in Figure 3.1, where θ_1 is the angle of the first pitch joint, θ_2 is the angle of the second pitch joint related to the first link, $m_1(m_2)$ is the mass of the link 1 (link 2), $l_1(l_2)$ is the length of the link 1 (link 2), and $\tau_1(\tau_2)$ is the actuated torque at the first pitch joint (second pitch joint) [16].

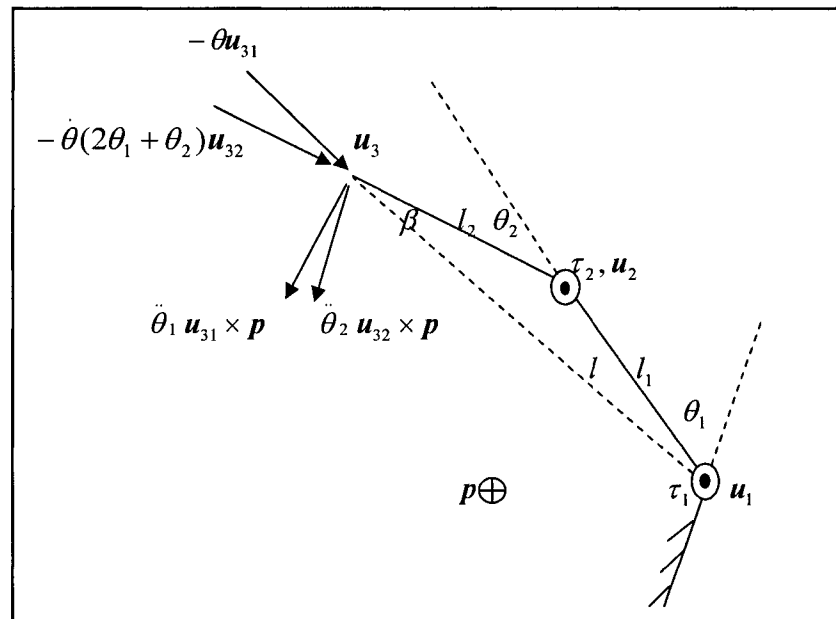


Figure 3.1 Model of a two-pitch-joint link system

The kinetic energy of the system, E_k , can be expressed as

$$E_k = \frac{1}{2}(m_1 + m_2)l_1^2 \left(\frac{d\theta_1}{dt}\right)^2 + \frac{1}{2}m_2 \left\{ l_2^2 \left(\frac{d\theta_1}{dt} + \frac{d\theta_2}{dt}\right)^2 + 2l_1 l_2 \frac{d\theta_1}{dt} \left(\frac{d\theta_1}{dt} + \frac{d\theta_2}{dt}\right) \cos \theta_2 \right\} \quad (3.1a)$$

The equations of motion of the system can be written as follows using Lagrangians:

$$(1 + \kappa \lambda^2 + 2\lambda \cos \theta_2) \ddot{\theta}_1 + (1 + \lambda \cos \theta_2) \ddot{\theta}_2 - \lambda \dot{\theta}_2 (2\dot{\theta}_1 + \dot{\theta}_2) \sin \theta_2 = \alpha \quad (3.2a)$$

$$(1 + \lambda \cos \theta_2) \ddot{\theta}_1 + \ddot{\theta}_2 + \lambda \dot{\theta}_1^2 \sin \theta_2 = \beta \quad (3.2b)$$

where

$$\kappa = \frac{m_1 + m_2}{m_2}, \lambda = \frac{l_1}{l_2},$$

$$\alpha = \frac{\tau_1}{m_2 g l_2}, \beta = \frac{\tau_2}{m_2 g l_2}$$

where g is the acceleration of gravity.

Equation (3.2a) and (3.2b) can also be written as:

$$\tau_1 = \frac{g}{l_2} \{ [m_1 l_1^2 + m_2 (l_1^2 + l_2^2 + 2l_1 l_2 \cos \theta_2)] \ddot{\theta}_1 + m_2 l_2 (l_1 \cos \theta_2 + l_2) \ddot{\theta}_2 - m_2 l_1 l_2 (2\dot{\theta}_1 + \dot{\theta}_2) \sin \theta_2 \dot{\theta}_2 \} \quad (3.2c)$$

$$\tau_2 = m_2 g \{ (l_1 \cos \theta_2 + l_2) \ddot{\theta}_1 + l_2 \ddot{\theta}_2 + l_1 \dot{\theta}_1^2 \sin \theta_2 \} \quad (3.2d)$$

In their paper, they chose the orientation as $\mathbf{p} = \begin{bmatrix} 0 \\ 0 \\ 1 \end{bmatrix}$, so there should be no gravity

terms in the equation. But in their equation, the gravity terms appear. This is an obvious error in the motion equation. In the next section, we will derive the motion equations and compare the difference.

3.2 Nonlinear State Space Equations

We do not exactly know how they derived the motion equations of the two-pitch-joint link system using Lagrangians since it is not discussed specifically in their paper. But we doubt the correctness of the motion equations. So there is a need to check their motion equations. However, we will derive our motion equations step by step first and then compare them with theirs.

From “Applied Robotic Analysis” (1991), the accelerations of end points of the link 1 (point \mathbf{u}_2) and link 2 (point \mathbf{u}_3) can be expressed as:

$$\ddot{\mathbf{u}}_2 = \ddot{\theta}_1 \mathbf{u}_{21} \times \mathbf{p} - \dot{\theta}_1^2 \mathbf{u}_{21} \quad (3.1)$$

$$\ddot{\mathbf{u}}_3 = \ddot{\theta}_1 \mathbf{u}_{31} \times \mathbf{p} + \ddot{\theta}_2 \mathbf{u}_{32} \times \mathbf{p} - \dot{\theta}_1^2 \mathbf{u}_{31} - \dot{\theta}_2^2 \mathbf{u}_{32} - 2\dot{\theta}_1 \dot{\theta}_2 \mathbf{u}_{32} \quad (3.2)$$

According to Newton’s second law, the forces on the point-mass m_1 at point \mathbf{u}_2 and m_2 at point \mathbf{u}_3 including gravity are:

$$\mathbf{f}_{m1} = m_1 \ddot{\mathbf{u}}_2 - m_1 \mathbf{g} \begin{bmatrix} 0 \\ 0 \\ 1 \end{bmatrix} \quad (3.3)$$

$$\mathbf{f}_{m2} = m_2 \ddot{\mathbf{u}}_3 - m_2 \mathbf{g} \begin{bmatrix} 0 \\ 0 \\ 1 \end{bmatrix} \quad (3.4)$$

The torque at \mathbf{u}_1 is produced by the component of the force orthogonal to \mathbf{u}_{31} . In this paper, we use τ_i to represent torques.

$$\begin{aligned} \tau_1 &= \mathbf{f}_{m1} \bullet \mathbf{u}_{21} \times \mathbf{p} + \mathbf{f}_{m2} \bullet \mathbf{u}_{31} \times \mathbf{p} \\ &= m_1 (\ddot{\mathbf{u}}_2 - \mathbf{g} \begin{bmatrix} 0 \\ 0 \\ 1 \end{bmatrix}) \bullet (\mathbf{u}_{21} \times \mathbf{p}) + m_2 (\ddot{\mathbf{u}}_3 - \mathbf{g} \begin{bmatrix} 0 \\ 0 \\ 1 \end{bmatrix}) \bullet (\mathbf{u}_{31} \times \mathbf{p}) \\ &= m_1 \{ \ddot{\theta}_1 \mathbf{u}_{21} \times \mathbf{p} - \dot{\theta}_1^2 \mathbf{u}_{21} - \mathbf{g} \begin{bmatrix} 0 \\ 0 \\ 1 \end{bmatrix} \} \bullet (\mathbf{u}_{21} \times \mathbf{p}) \\ &\quad + m_2 \{ \ddot{\theta}_1 \mathbf{u}_{31} \times \mathbf{p} + \ddot{\theta}_2 \mathbf{u}_{32} \times \mathbf{p} - \dot{\theta}_1^2 \mathbf{u}_{31} - \dot{\theta}_2^2 \mathbf{u}_{32} - 2\dot{\theta}_1 \dot{\theta}_2 \mathbf{u}_{32} - \mathbf{g} \begin{bmatrix} 0 \\ 0 \\ 1 \end{bmatrix} \} \bullet (\mathbf{u}_{31} \times \mathbf{p}) \end{aligned} \quad (3.5)$$

Also, as noted in Chapter 2, there may be some simplifications made to the terms involving gravity when an orientation is chosen for the chain of links and joints. For

example, suppose $\mathbf{p} = \begin{bmatrix} 0 \\ 0 \\ 1 \end{bmatrix}$, the gravity terms drop out in equation (3.5). Neglect detail

calculation, equation (3.5) becomes

$$\begin{aligned} \tau_1 = m_1 \ddot{\theta}_1 l_1^2 \\ + m_2 \{ \ddot{\theta}_1 l_1^2 + \ddot{\theta}_2 l_2 \cos \beta - l_2 \sin \beta \dot{\theta}_2^2 - 2l_2 \sin \beta \dot{\theta}_1 \dot{\theta}_2 \} \end{aligned} \quad (3.6)$$

l is the distance between point \mathbf{u}_1 and point \mathbf{u}_3 ; l_1 is the distance between point \mathbf{u}_1 and point \mathbf{u}_2 (the length of rigid link 1); l_2 is the distance between point \mathbf{u}_2 and point \mathbf{u}_3 (the length of rigid link 2); β is the angle between l and l_2 . According to the law of sines and law of cosines, we can get

$$l = |\mathbf{u}_{31}| = \sqrt{l_1^2 + l_2^2 + 2l_1 l_2 \cos \theta_2} \quad (3.7)$$

Therefore,

$$l^2 = l_1^2 + l_2^2 + 2l_1 l_2 \cos \theta_2 \quad (3.8)$$

According to law of sines,

$$\frac{l_1}{\sin \beta} = \frac{l}{\sin(\pi - \theta_2)} = \frac{l}{\sin \theta_2} \quad (3.9)$$

$$\sin \beta = \frac{l_1 \sin \theta_2}{l} \quad (3.10)$$

From equation (3.10),

$$\sin^2 \beta = \frac{l_1^2 \sin^2 \theta_2}{l^2} \quad (3.11)$$

$$\cos \beta = \sqrt{1 - \sin^2 \beta} \quad (3.12)$$

Putting equation (3.11) into equation (3.12) and simplifying it gives,

$$\cos \beta = \sqrt{1 - \frac{l_1^2 \sin^2 \theta_2}{l^2}} = \frac{1}{l} \sqrt{l^2 - l_1^2 \sin^2 \theta_2} = \frac{1}{l} \sqrt{(l_1 \cos \theta_2 + l_2)^2} = \frac{l_1 \cos \theta_2 + l_2}{l} \quad (3.13)$$

So the actuated torque at u_1 is

$$\begin{aligned} \tau_1 = & [m_1 l_1^2 + m_2 (l_1^2 + l_2^2 + 2l_1 l_2 \cos \theta_2)] \ddot{\theta}_1 + m_2 l_2 (l_1 \cos \theta_2 + l_2) \ddot{\theta}_2 \\ & - m_2 l_1 l_2 (2\dot{\theta}_1 + \dot{\theta}_2) \sin \theta_2 \dot{\theta}_2 \end{aligned} \quad (3.14)$$

We will get the actuated torque at u_2 (τ_2) using the same method:

$$\begin{aligned} \tau_2 = & \mathbf{f}_{m_2} \bullet \mathbf{u}_{31} \times \mathbf{p} \\ = & m_2 (\ddot{\mathbf{u}}_3 - \mathbf{g}) \bullet (\mathbf{u}_{31} \times \mathbf{p}) \\ = & m_2 \left\{ \ddot{\theta}_1 \mathbf{u}_{31} \times \mathbf{p} + \ddot{\theta}_2 \mathbf{u}_{32} \times \mathbf{p} - \dot{\theta}_1^2 \mathbf{u}_{31} - \dot{\theta}_2^2 \mathbf{u}_{32} - 2\dot{\theta}_1 \dot{\theta}_2 \mathbf{u}_{32} - \mathbf{g} \right\} \bullet (\mathbf{u}_{32} \times \mathbf{p}) \end{aligned} \quad (3.15)$$

Putting equation (3.13) into equation (3.15) gives,

$$\tau_2 = m_2 \{ l_2 (l_1 \cos \theta_2 + l_2) \ddot{\theta}_1 + l_2^2 \ddot{\theta}_2 + l_1 l_2 \dot{\theta}_1^2 \sin \theta_2 \} \quad (3.16)$$

Equations (3.14) and (3.16) constitute a nonlinear second-order differential equation

group in the case of $\mathbf{p} = \begin{bmatrix} 0 \\ 0 \\ 1 \end{bmatrix}$.

Next, suppose $\mathbf{p} = \begin{bmatrix} 0 \\ 1 \\ 0 \end{bmatrix}$, neglect detail calculation, equation (3.5) becomes the final

form:

$$\begin{aligned} \tau_1 = & [m_1 l_1^2 + m_2 (l_1^2 + l_2^2 + 2l_1 l_2 \cos \theta_2)] \ddot{\theta}_1 + m_2 l_2 (l_1 \cos \theta_2 + l_2) \ddot{\theta}_2 \\ & - m_2 l_1 l_2 (2\dot{\theta}_1 + \dot{\theta}_2) \sin \theta_2 \dot{\theta}_2 - m_1 g l_1 \sin \theta_1 - m_2 g [l_1 \sin \theta_1 + l_2 \sin(\theta_1 + \theta_2)] \end{aligned} \quad (3.17)$$

Using the same method, neglect detail calculation, equation (3.15) becomes the final

form:

$$\tau_2 = m_2 \{l_2 (l_1 \cos \theta_2 + l_2) \ddot{\theta}_1 + l_2^2 \ddot{\theta}_2 + l_1 l_2 \dot{\theta}_1^2 \sin \theta_2 - g l_2 \sin(\theta_1 + \theta_2)\} \quad (3.18)$$

Equations (3.17) and (3.18) constitute a nonlinear second-order differential equation

group in the case of $\mathbf{p} = \begin{bmatrix} 0 \\ 1 \\ 0 \end{bmatrix}$.

As noted before in this section, we will compare the motion equations of Kee-Ho Yu's and that of ours. In Kee-Ho Yu's paper, the horizontal orientation is chosen for

this system. That is, $\mathbf{p} = \begin{bmatrix} 0 \\ 0 \\ 1 \end{bmatrix}$ is chosen. So we will only compare equations (3.2c) and

(3.2d) with equations (3.14) and (3.16) respectively. From equation (3.2c) and equation (3.14), we can see that right sides of both equations are the same except that

the first term of the right side of equation (3.2c) is $\frac{g}{l_2}$ while the first term of the right

side of equation (3.14) is "1". From equation (3.2d) and equation (3.16), we can see the only difference is that the first term of right side of equation (3.2d) is $m_2 g$ while

the first term of the right side of equation (3.16) is $m_2 l_2$. Since $\mathbf{p} = \begin{bmatrix} 0 \\ 0 \\ 1 \end{bmatrix}$ is chosen for

this system, the gravity terms drop out. But in Kee-Ho Yu's equations, there are terms involving gravity. That proves that their equations are not correct.

In these two equation groups, τ_1 and τ_2 are input variables, θ_1, θ_2 are output variables, other parameters are constants. The objective for us is to find the dynamic characteristics of this two-pitch-joint link system, that is, relationship between the torque space and the joint space. That means we should try to find the analytical solution of these two nonlinear second-order differential equation groups. Also, as

discussed in Chapter 2, through observation we find that it is impractical to find the analytical solutions of these two equation groups. The only method to solve this problem is numerical solution. As for this system, it is a kind of initial value problems. Be the same as Chapter 2, the techniques applicable to initial value problems are designed to solve the following n-dimensional nonlinear first order system of ordinary differential equations over the specified time interval $\alpha \leq t \leq \beta$.

$$\frac{d}{dt} \underline{z} = \underline{f}(\underline{z}, \underline{u}, t) \quad (3.19)$$

Equation (3.19) is called standard state form. So if we want to get the numerical solution of this ordinary differential equation group, we need put it into standard state form.

First, consider equations (3.14) and (3.16). That is, consider the case of $\underline{p} = \begin{bmatrix} 0 \\ 0 \\ 1 \end{bmatrix}$. To

put them into standard state form, we should first manipulate the equations algebraically to only have a single second derivative term in each equation. From equation (3.16), we have

$$\ddot{\theta}_2 = \frac{1}{m_2 l_2^2} [\tau_2 - m_2 l_2 (l_1 \cos \theta_2 + l_2) \ddot{\theta}_1 - m_2 l_1 l_2 \dot{\theta}_1^2 \sin \theta_2] \quad (3.20)$$

and putting this into equation (3.14) gives,

$$\begin{aligned} l_1^2 l_2 (m_1 + m_2 \sin^2 \theta_2) \ddot{\theta}_1 &= l_2 \tau_1 - (l_1 \cos \theta_2 + l_2) \tau_2 + m_2 l_1 l_2 (l_1 \cos \theta_2 + l_2) \dot{\theta}_1^2 \sin \theta_2 \\ &\quad + m_2 l_1 l_2^2 (2\dot{\theta}_1 + \dot{\theta}_2) \sin \theta_2 \dot{\theta}_2 \end{aligned} \quad (3.21)$$

From equation (3.16),

$$\ddot{\theta}_1 = \frac{\tau_2 - m_2 l_2^2 \ddot{\theta}_2 - m_2 l_1 l_2 \dot{\theta}_1^2 \sin \theta_2}{m_2 l_2 (l_1 \cos \theta_2 + l_2)} \quad (3.22)$$

putting this into equation (3.14) gives,

$$\begin{aligned}
l_1^2 l_2^2 m_2 (m_1 + m_2 \sin^2 \theta_2) \ddot{\theta}_2 = & -m_2 l_2 (l_1 \cos \theta_2 + l_2) \tau_1 + (m_1 l_1^2 + m_2 l_1^2 + m_2 l_2^2 + 2m_2 l_1 l_2 \cos \theta_2) \\
& (\tau_2 - m_2 l_1 l_2 \dot{\theta}_1^2 \sin \theta_2) - m_2^2 l_1 l_2^2 (l_1 \cos \theta_2 + l_2) \\
& (2\dot{\theta}_1 + \dot{\theta}_2) \sin \theta_2 \dot{\theta}_2
\end{aligned} \tag{3.23}$$

Finally, dividing by the lead coefficient of the equations (3.21) and (3.23) gives,

$$\begin{aligned}
\ddot{\theta}_1 = & \frac{1}{l_1^2 l_2 (m_1 + m_2 \sin^2 \theta_2)} \{l_2 \tau_1 - (l_1 \cos \theta_2 + l_2) \tau_2 + m_2 l_1 l_2 (l_1 \cos \theta_2 + l_2) \dot{\theta}_1^2 \sin \theta_2 \\
& + m_2 l_1 l_2^2 (2\dot{\theta}_1 + \dot{\theta}_2) \sin \theta_2 \dot{\theta}_2\}
\end{aligned} \tag{3.24}$$

$$\begin{aligned}
\ddot{\theta}_2 = & \frac{1}{m_2 (m_1 + m_2 \sin^2 \theta_2) l_1^2 l_2^2} \{-m_2 l_2 (l_1 \cos \theta_2 + l_2) \tau_1 + (m_1 l_1^2 + m_2 l_1^2 + m_2 l_2^2 + \\
& 2m_2 l_1 l_2 \cos \theta_2) (\tau_2 - m_2 l_1 l_2 \dot{\theta}_1^2 \sin \theta_2) - m_2^2 l_1 l_2^2 (l_1 \cos \theta_2 + l_2) \\
& (2\dot{\theta}_1 + \dot{\theta}_2) \sin \theta_2 \dot{\theta}_2\}
\end{aligned} \tag{3.25}$$

Next, consider equations (3.17) and (3.18). That is, consider the case of $\mathbf{p} = \begin{bmatrix} 0 \\ 1 \\ 0 \end{bmatrix}$. To

put them into standard state form, we should first manipulate the equations algebraically to only have a single second derivative term in each equation. From equation (3.18), we have

$$\ddot{\theta}_2 = \frac{1}{m_2 l_2^2} [\tau_2 - m_2 l_2 (l_1 \cos \theta_2 + l_2) \ddot{\theta}_1 - m_2 l_1 l_2 \dot{\theta}_1^2 \sin \theta_2 + m_2 g l_2 \sin(\theta_1 + \theta_2)] \tag{3.26}$$

and putting this into equation (3.17) gives

$$\begin{aligned}
l_1^2 l_2 (m_1 + m_2 \sin^2 \theta_2) \ddot{\theta}_1 = & l_2 \tau_1 - (l_1 \cos \theta_2 + l_2) \tau_2 + m_2 l_1 l_2 (l_1 \cos \theta_2 + l_2) \dot{\theta}_1^2 \sin \theta_2 \\
& - m_2 g l_2 (l_1 \cos \theta_2 + l_2) \sin(\theta_1 + \theta_2) + m_2 l_1 l_2^2 (2\dot{\theta}_1 + \dot{\theta}_2) \sin \theta_2 \dot{\theta}_2 \\
& + m_1 g l_1 l_2 \sin \theta_1 + m_2 g l_2 [l_1 \sin \theta_1 + l_2 \sin(\theta_1 + \theta_2)]
\end{aligned} \tag{3.27}$$

From equation (3.18),

$$\ddot{\theta}_1 = \frac{\tau_2 - m_2 l_2^2 \ddot{\theta}_2 - m_2 l_1 l_2 \dot{\theta}_1^2 \sin \theta_2 + m_2 g l_2 \sin(\theta_1 + \theta_2)}{m_2 l_2 (l_1 \cos \theta_2 + l_2)} \quad (3.28)$$

putting this into equation (3.17) gives

$$\begin{aligned} l_1^2 l_2^2 m_2 (m_1 + m_2 \sin^2 \theta_2) \ddot{\theta}_2 = & -m_2 l_2 (l_1 \cos \theta_2 + l_2) \tau_1 + (m_1 l_1^2 + m_2 l_1^2 + m_2 l_2^2 + 2m_2 l_1 l_2 \cos \theta_2) \\ & [\tau_2 - m_2 l_1 l_2 \dot{\theta}_1^2 \sin \theta_2 + m_2 g l_2 \sin(\theta_1 + \theta_2)] - m_2^2 l_1 l_2^2 (l_1 \cos \theta_2 + l_2) \\ & (2\dot{\theta}_1 + \dot{\theta}_2) \sin \theta_2 \dot{\theta}_2 - m_1 m_2 g l_1 l_2 (l_1 \cos \theta_2 + l_2) \sin \theta_1 \\ & - m_2^2 g l_2 (l_1 \cos \theta_2 + l_2) [l_1 \sin \theta_1 + l_2 \sin(\theta_1 + \theta_2)] \end{aligned} \quad (3.29)$$

Finally, dividing by the lead coefficient of the equations (3.27) and (3.29) gives,

$$\begin{aligned} \ddot{\theta}_1 = & \frac{1}{l_1^2 l_2 (m_1 + m_2 \sin^2 \theta_2)} \{ l_2 \tau_1 - (l_1 \cos \theta_2 + l_2) \tau_2 + m_2 l_1 l_2 (l_1 \cos \theta_2 + l_2) \dot{\theta}_1^2 \sin \theta_2 \\ & - m_2 g l_2 (l_1 \cos \theta_2 + l_2) \sin(\theta_1 + \theta_2) + m_2 l_1 l_2^2 (2\dot{\theta}_1 + \dot{\theta}_2) \sin \theta_2 \dot{\theta}_2 + m_1 g l_1 l_2 \sin \theta_1 \\ & + m_2 g l_2 [l_1 \sin \theta_1 + l_2 \sin(\theta_1 + \theta_2)] \} \end{aligned} \quad (3.30)$$

$$\begin{aligned} \ddot{\theta}_2 = & \frac{1}{m_2 (m_1 + m_2 \sin^2 \theta_2) l_1^2 l_2^2} \{ -m_2 l_2 (l_1 \cos \theta_2 + l_2) \tau_1 + (m_1 l_1^2 + m_2 l_1^2 + m_2 l_2^2 + \\ & 2m_2 l_1 l_2 \cos \theta_2) [\tau_2 - m_2 l_1 l_2 \dot{\theta}_1^2 \sin \theta_2 + m_2 g l_2 \sin(\theta_1 + \theta_2)] - m_2^2 l_1 l_2^2 (l_1 \cos \theta_2 + l_2) \\ & (2\dot{\theta}_1 + \dot{\theta}_2) \sin \theta_2 \dot{\theta}_2 - m_1 m_2 g l_1 l_2 (l_1 \cos \theta_2 + l_2) \sin \theta_1 - m_2^2 g l_2 (l_1 \cos \theta_2 + l_2) \\ & [l_1 \sin \theta_1 + l_2 \sin(\theta_1 + \theta_2)] \} \end{aligned} \quad (3.31)$$

Now, put these equations of two cases into standard state form. We make the following substitutions:

$$z_1 = \theta_1 \quad z_2 = \dot{\theta}_1 = \dot{z}_1 \quad z_3 = \theta_2 \quad z_4 = \dot{\theta}_2 = \dot{z}_3 \quad (3.32)$$

In the case of $p = \begin{bmatrix} 0 \\ 0 \\ 1 \end{bmatrix}$, write the final state space equation for the two pitch joint

system as

$$\frac{d}{dt} \underline{z} = \frac{d}{dt} \begin{bmatrix} z_1 \\ z_2 \\ z_3 \\ z_4 \end{bmatrix} = \begin{bmatrix} z_2 \\ \frac{1}{l_1^2 l_2 (m_1 + m_2 \sin^2 z_3)} \{ l_2 \tau_1 - (l_1 \cos z_3 + l_2) \tau_2 + m_2 l_1 l_2 (l_1 \cos z_3 + l_2) z_2^2 \sin z_3 \\ + m_2 l_1 l_2^2 (2z_2 + z_4) (\sin z_3) z_4 \} \\ z_4 \\ \frac{1}{l_1^2 l_2^2 m_2 (m_1 + m_2 \sin^2 z_3)} \{ -m_2 l_2 (l_1 \cos z_3 + l_2) \tau_1 + (m_1 l_1^2 + m_2 l_1^2 + m_2 l_2^2 \\ + 2m_2 l_1 l_2 \cos z_3) (\tau_2 - m_2 l_1 l_2 z_2^2 \sin z_3) - m_2^2 l_1 l_2^2 (l_1 \cos z_3 + l_2) \\ (2z_2 + z_4) (\sin z_3) z_4 \} \end{bmatrix} \quad (3.33)$$

In the case of $\underline{p} = \begin{bmatrix} 0 \\ 1 \\ 0 \end{bmatrix}$, write the final state space equation for the two pitch joint

system as

$$\frac{d}{dt} \underline{z} = \frac{d}{dt} \begin{bmatrix} z_1 \\ z_2 \\ z_3 \\ z_4 \end{bmatrix} = \begin{bmatrix} z_2 \\ \frac{1}{l_1^2 l_2 (m_1 + m_2 \sin^2 z_3)} \{ l_2 \tau_1 - (l_1 \cos z_3 + l_2) \tau_2 + m_2 l_1 l_2 (l_1 \cos z_3 + l_2) z_2^2 \sin z_3 \\ - m_2 g l_2 (l_1 \cos z_3 + l_2) \sin(z_1 + z_3) + m_2 l_1 l_2^2 (2z_2 + z_4) (\sin z_3) z_4 \\ + m_1 g l_1 l_2 \sin z_1 + m_2 g l_2 [l_1 \sin z_1 + l_2 \sin(z_1 + z_3)] \} \\ z_4 \\ \frac{1}{l_1^2 l_2^2 m_2 (m_1 + m_2 \sin^2 z_3)} \{ -m_2 l_2 (l_1 \cos z_3 + l_2) \tau_1 + (m_1 l_1^2 + m_2 l_1^2 + m_2 l_2^2 \\ + 2m_2 l_1 l_2 \cos z_3) [\tau_2 - m_2 l_1 l_2 z_2^2 \sin z_3 + m_2 g l_2 \sin(z_1 + z_3)] \\ - m_2^2 l_1 l_2^2 (l_1 \cos z_3 + l_2) (2z_2 + z_4) (\sin z_3) z_4 - m_1 m_2 g l_1 l_2 (l_1 \cos z_3 + l_2) \sin z_1 \\ - m_2^2 g l_2 (l_1 \cos z_3 + l_2) [l_1 \sin z_1 + l_2 \sin(z_1 + z_3)] \} \end{bmatrix} \quad (3.34)$$

These two expressions are the desired forms given in equation (3.19) in the cases

$$\text{of } \underline{p} = \begin{bmatrix} 0 \\ 0 \\ 1 \end{bmatrix} \text{ and } \underline{p} = \begin{bmatrix} 0 \\ 1 \\ 0 \end{bmatrix} \text{ respectively.}$$

Again, we will simulate the two cases of this system in Matlab using its ODE routines such as ode23, and discuss the dynamic characteristics of this system in following sections

3.3 Characteristics in Free Motion

In this section, we will discuss the characteristics in free motion of the vertical two-pitch-joint link system. Two cases will be studied. One is in case of $\underline{p} = [0 \ 0 \ 1]^T$; and the other is in case of $\underline{p} = [0 \ 1 \ 0]^T$. In case of $\underline{p} = [0 \ 0 \ 1]^T$, the free motion can

be classified into two types according the different initial conditions. The one is rotation and the other is oscillation.

In free motion, the actuated torques equal zero and the kinetic energy is a constant.

Let the actuated torques be $\tau_i, i = 1, 2$. So $\tau_1 = \tau_2 = 0$; Let the kinetic energy be E_{k_c} . Here

$$E_{k_c} = C, C \text{ is a constant.}$$

3.3.1 Characteristics in Free Motion in Case of $p = [0 \ 0 \ 1]^T$

In this case, the free motion can be classified into two types according to the different initial conditions. One is rotation and the other is oscillation. Furthermore, we know that the angular velocity of this system (or the kinetic energy of this system) determines which motion will appear.

Simulate the two-pitch-joint link system using different physical parameters which are listed in Table 3.1 under certain initial conditions. We simulate this system according to state space equation (3.33) within Matlab using its ode23 routine under different initial conditions.

Table 3.1 Physical parameters of a two-pitch-joint link system

k_1	0.1	1	10
k_2	0.1	1	10

$$\text{Note: } k_1 = \frac{m_1}{m_2}, k_2 = \frac{l_1}{l_2}$$

From the simulation results, we can see that second link of this system keeps rotating or oscillating according to different physical parameters and different initial conditions. It is hard to summarize rule of classification of motion mode because we have no analytical solutions to this system. This is the disadvantage of numerical

solution which is used in this paper. However it is the only choice when analytical solution is not practical and it is a strong tool to solve a specific problem. We can still find the following characteristics about the free motion:

- 1) If the second link of the system keeps oscillating, when k_2 (the ration of l_1 and l_2) is fixed, the amplitude of the oscillating increases while k_1 (the ratio of m_1 and m_2) increases.
- 2) If the second link of the system keeps rotating, when k_2 (the ration of l_1 and l_2) is fixed, the rotating displacement increases while k_1 (the ratio of m_1 and m_2) increases.

We can only try finite scenario which can not include all cases of realistic problems. Next, we will give two examples which represent two types of free motion. Example 1 represents oscillation type and example 2 represents rotation type.

Example 1, assume $m_1 = m_2 = 1kg$ and $l_1 = l_2 = 1m$. Simulate this two-pitch-joint link

system under the following initial condition: $\underline{z}_0 = \begin{bmatrix} 0 \\ 1 \\ 0 \\ 1 \end{bmatrix}$. We will simulate this system

according to the state space equation (3.33) within Matlab using its ode23 routine. Figure 3.2 and Figure 3.3 represent the relationships of 1st and 2nd joint angular displacement versus time respectively.

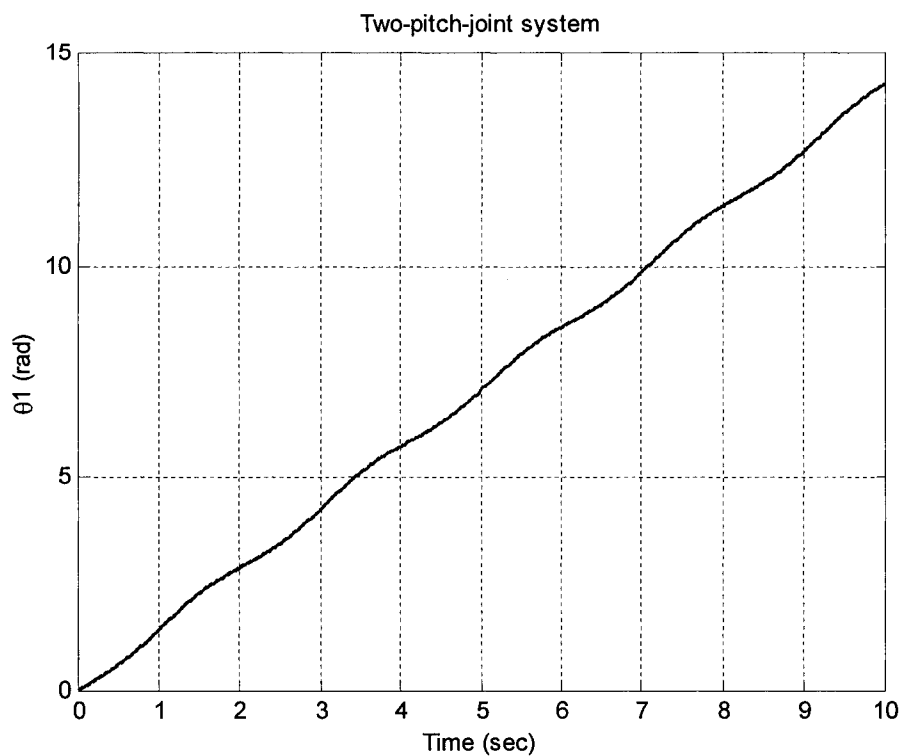


Figure 3.2 1st joint angular displacement versus time at the initial condition:
 $\tau_1 = 0, \tau_2 = 0, \underline{z}_0 = [0 \ 1 \ 0 \ 1]^T$

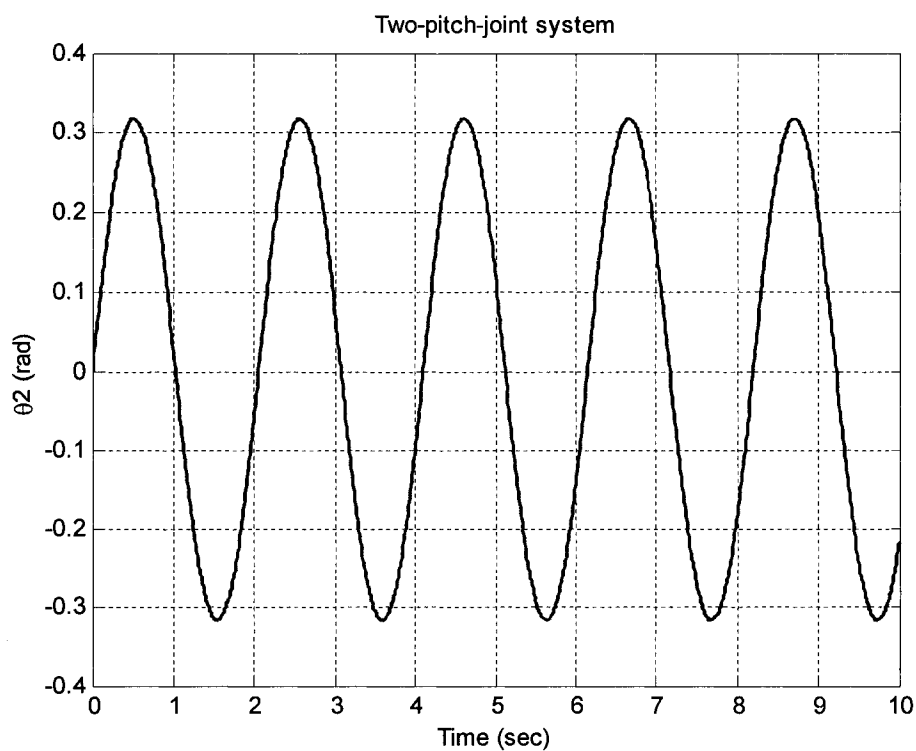


Figure 3.3 2nd joint angular displacement versus time at the initial condition:
 $\tau_1 = 0, \tau_2 = 0, \underline{z}_0 = [0 \ 1 \ 0 \ 1]^T$

From Figure 3.2 and Figure 3.3, we can see that the first link rotates continuously while the second link oscillates between two specified points. In free motion, there is no actuated torques acting on the system. So the kinetic energy of this system is a constant. It can be verified from Figure 3.2 through Figure 3.5. Figure 3.4 and Figure 3.5 are the plots that represent relationship of first and second joint angular velocities versus time respectively.

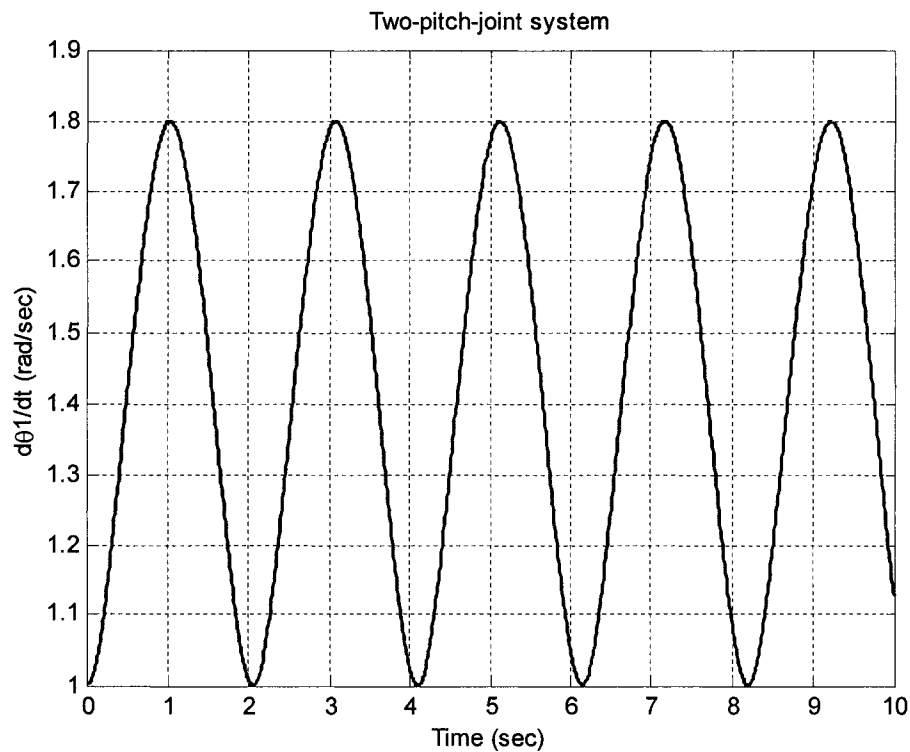


Figure 3.4 1st joint angular velocity versus time at the initial condition:
 $\tau_1 = 0, \tau_2 = 0, \underline{z}_0 = [0 \ 1 \ 0 \ 1]^T$

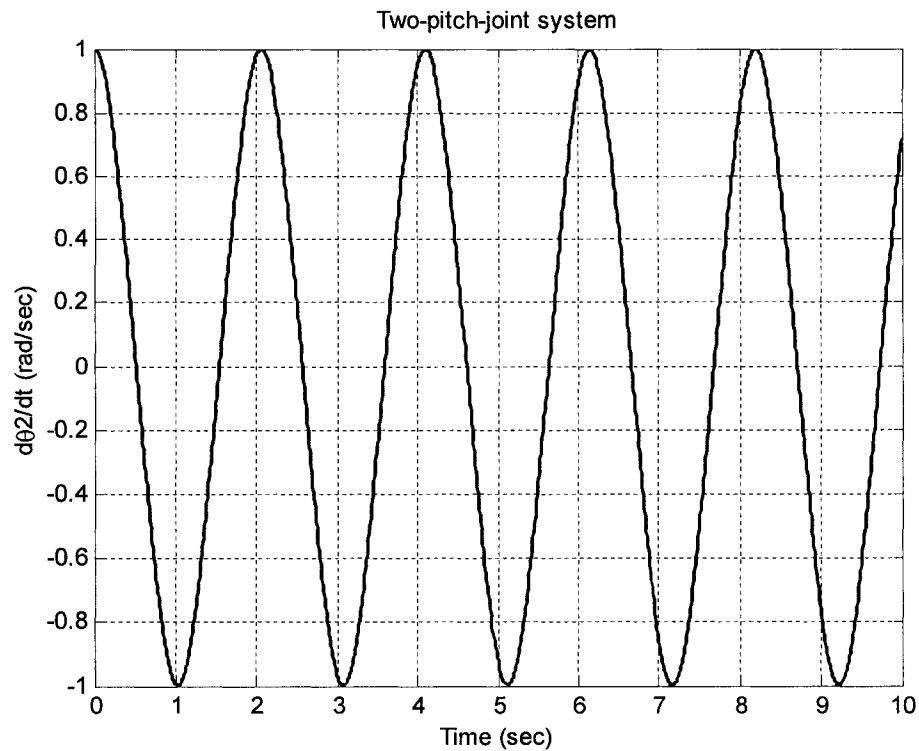


Figure 3.5 2nd joint angular velocity versus time at the initial condition:
 $\tau_1 = 0, \tau_2 = 0, \underline{z}_0 = [0 \ 1 \ 0 \ 1]^T$

Because there is a relative motion between 1st link and 2nd link, there exists relative angular acceleration between 1st link and 2nd link. Figure 3.6 and Figure 3.7 are the plots that represent relationship of first and second joint angular accelerations versus time respectively. The first joint angular acceleration is absolute angular acceleration while the second joint angular acceleration is relative angular acceleration to the first link.

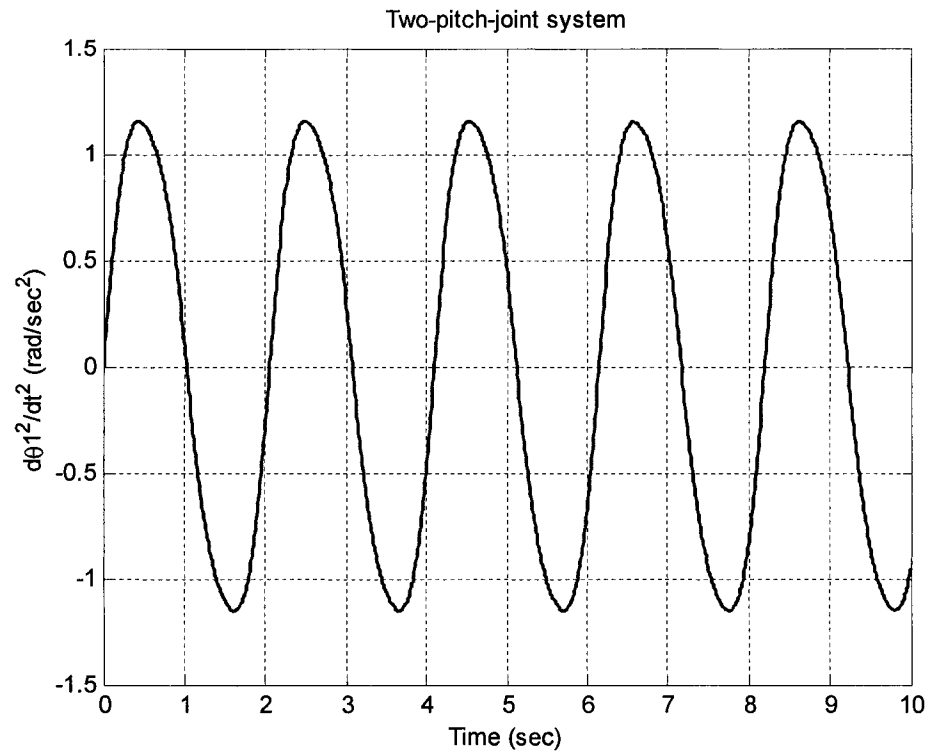


Figure 3.6 1st joint angular acceleration versus time at the initial condition:
 $\tau_1 = 0, \tau_2 = 0, \underline{z}_0 = [0 \ 1 \ 0 \ 1]^T$

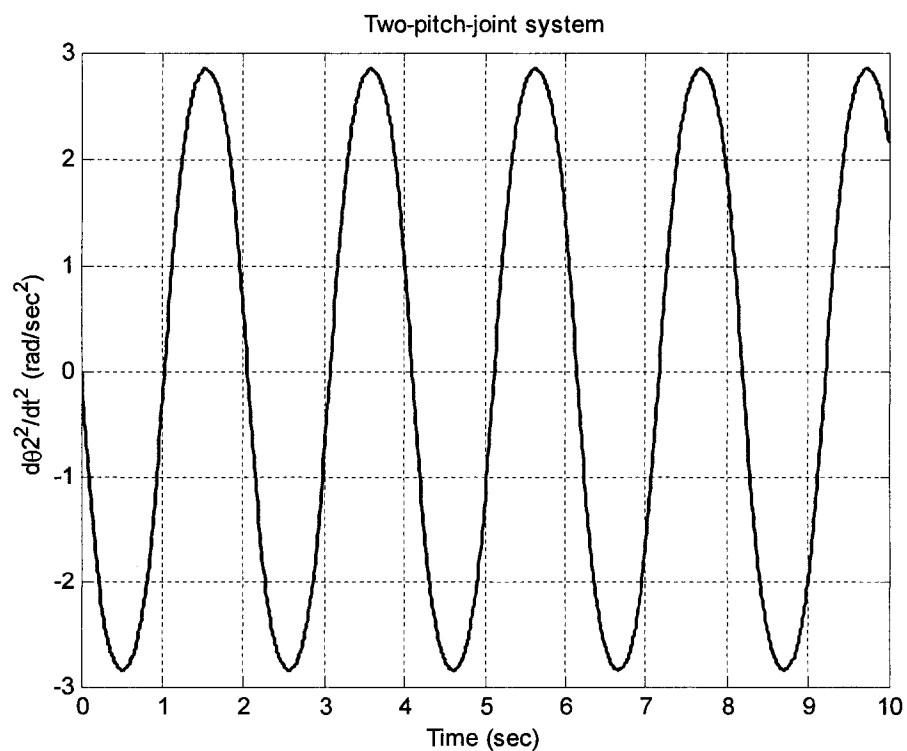


Figure 3.7 2nd joint angular acceleration versus time at the initial condition:
 $\tau_1 = 0, \tau_2 = 0, \underline{z}_0 = [0 \ 1 \ 0 \ 1]^T$

In addition, From Figure 3.3, Figure 3.5 and Figure 3.7, the numerical solution curves look like sine waves. Let's compare the numerical solution curves with the corresponding sine waves. Figure 3.8 through Figure 3.10 are the comparison results. The comparisons are almost the same. Meanwhile, we calculate the relative error of each solution curve which is about $\pm 3\%$, $\pm 4\%$, $\pm 5\%$ respectively. It suggests that the solution curves can be treated as sine waves under certain initial condition. Further, we need prove it through analytical method. It exceeds the focus of this thesis.

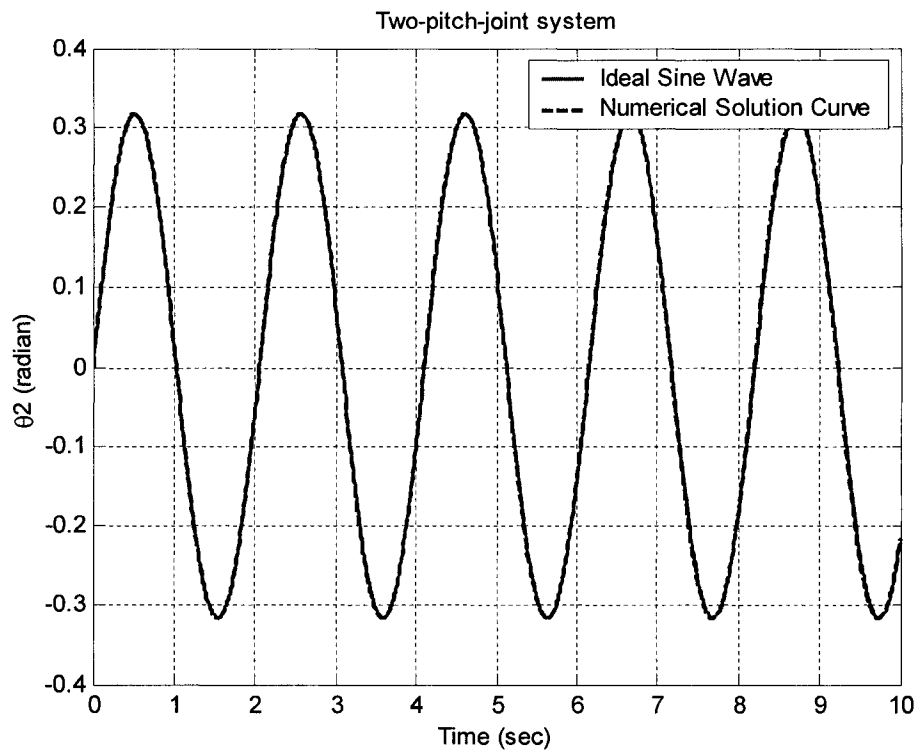


Figure 3.8 Comparison between numerical solution curve and the corresponding sine wave of 2nd joint angular displacement

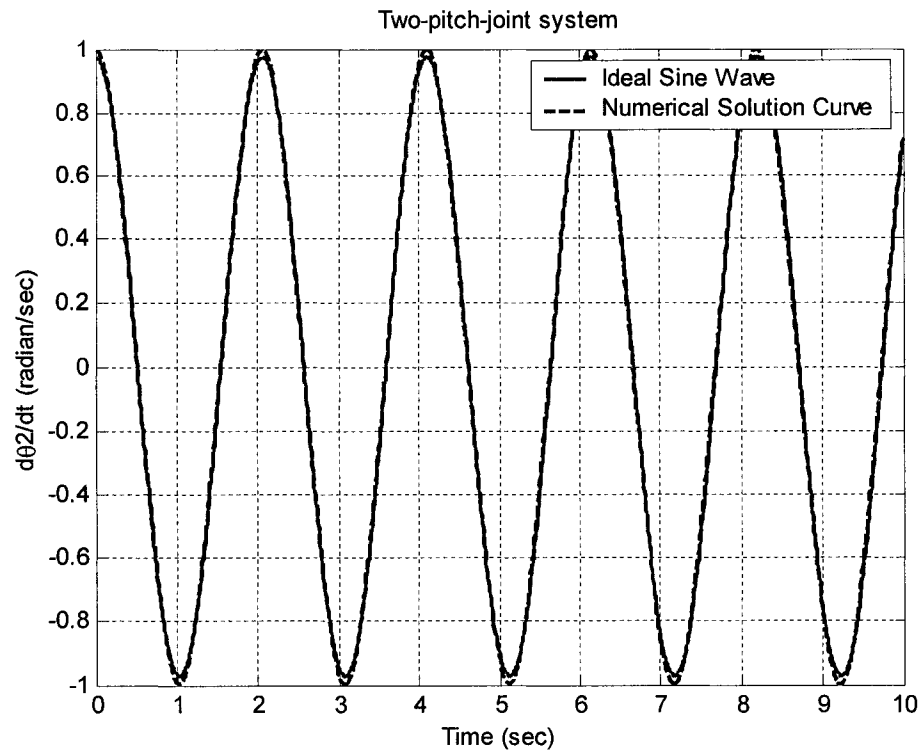


Figure 3.9 Comparison between numerical solution curve and the corresponding sine wave of 2nd joint angular velocity

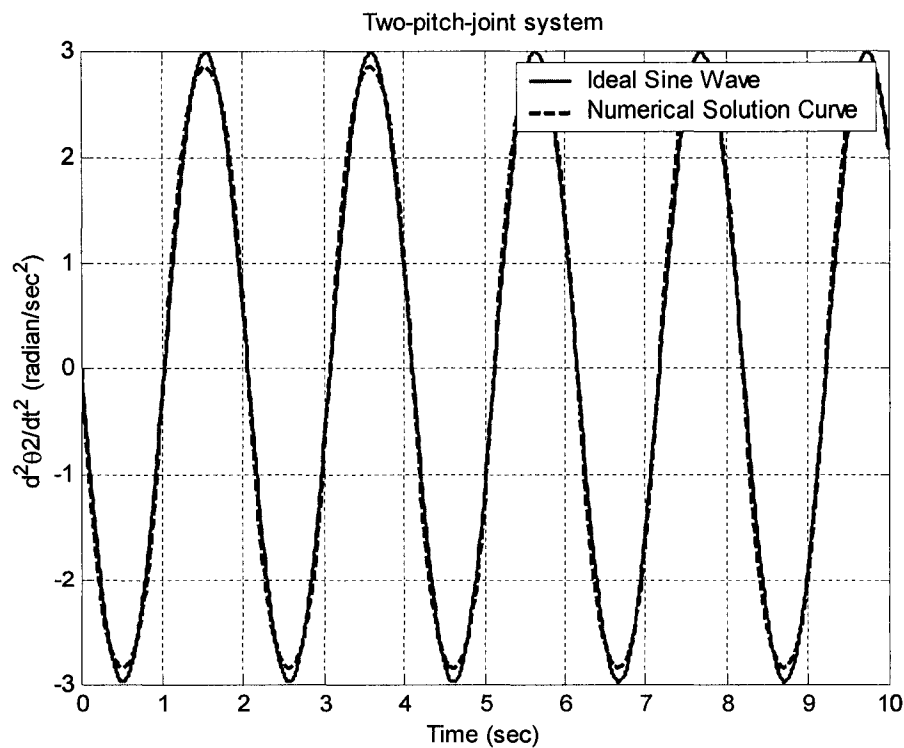


Figure 3.10 Comparison between numerical solution curve and the corresponding sine wave of 2nd joint angular acceleration

Example 2, assume $m_1 = 10\text{kg}$, $m_2 = 1\text{kg}$ and $l_1 = 0.1\text{m}$, $l_2 = 1\text{m}$. Simulate this two-

pitch-joint link system under the following initial condition: $\underline{z}_0 = \begin{bmatrix} 0 \\ 1 \\ 0 \\ -1 \end{bmatrix}$. We will

simulate this system according to the state space equation (3.33) within Matlab using its ode23 routine. Figure 3.11 and Figure 3.12 are the plots that represent the relationship of first and second joint angular displacement versus time respectively.

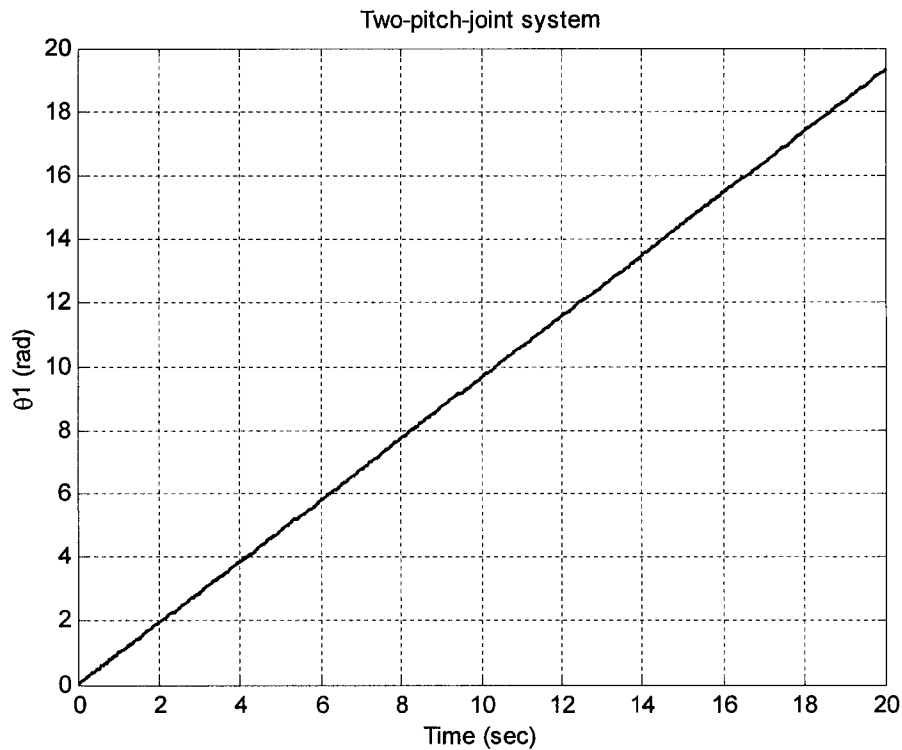


Figure 3.11 1st joint angular displacement versus time at the initial condition:

$$\tau_1 = 0, \tau_2 = 0, \underline{z}_0 = [0 \quad 1 \quad 0 \quad -1]'$$

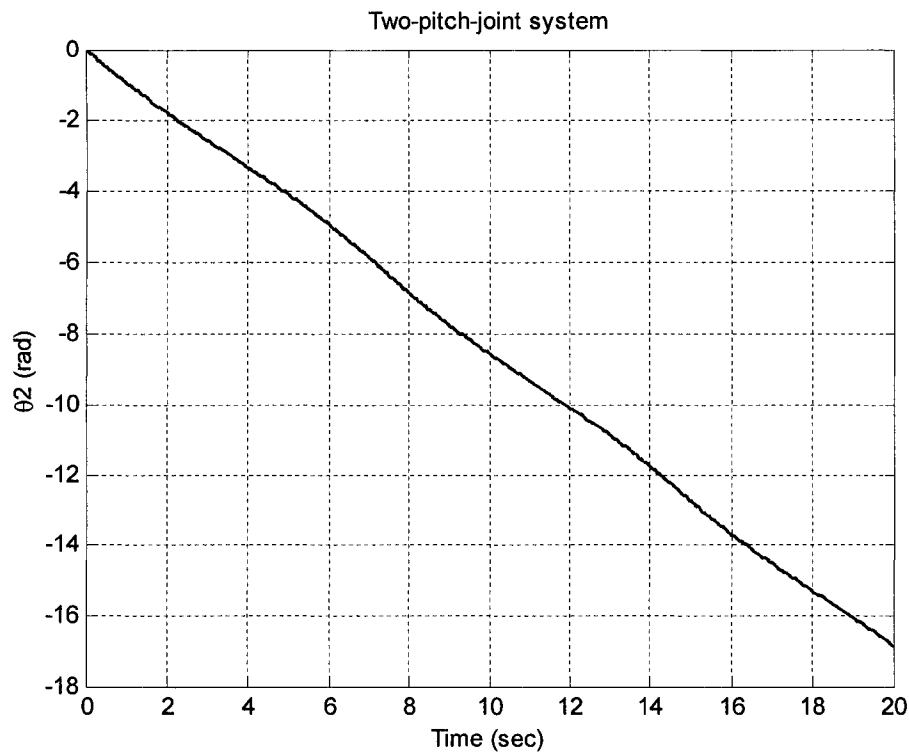


Figure 3.12 2nd joint angular displacement versus time at the initial condition:
 $\tau_1 = 0, \tau_2 = 0, z_0 = [0 \ 1 \ 0 \ -1]'$

From Figure 3.11 and Figure 3.12, it can be seen that the first link rotates counterclockwise continuously while the second link rotates clockwise continuously. Figure 3.13 and Figure 3.14 are the plots that represent the relationships of 1st and 2nd joint angular velocities versus time respectively. Again since there is a relative motion between 1st link and 2nd link, there exists relative angular acceleration between 1st link and 2nd link. Figure 3.15 and Figure 3.16 are the plots that represent relationship of first and second joint angular accelerations versus time respectively. The first joint angular acceleration is absolute angular acceleration while the second joint angular acceleration is relative angular acceleration to the first link.

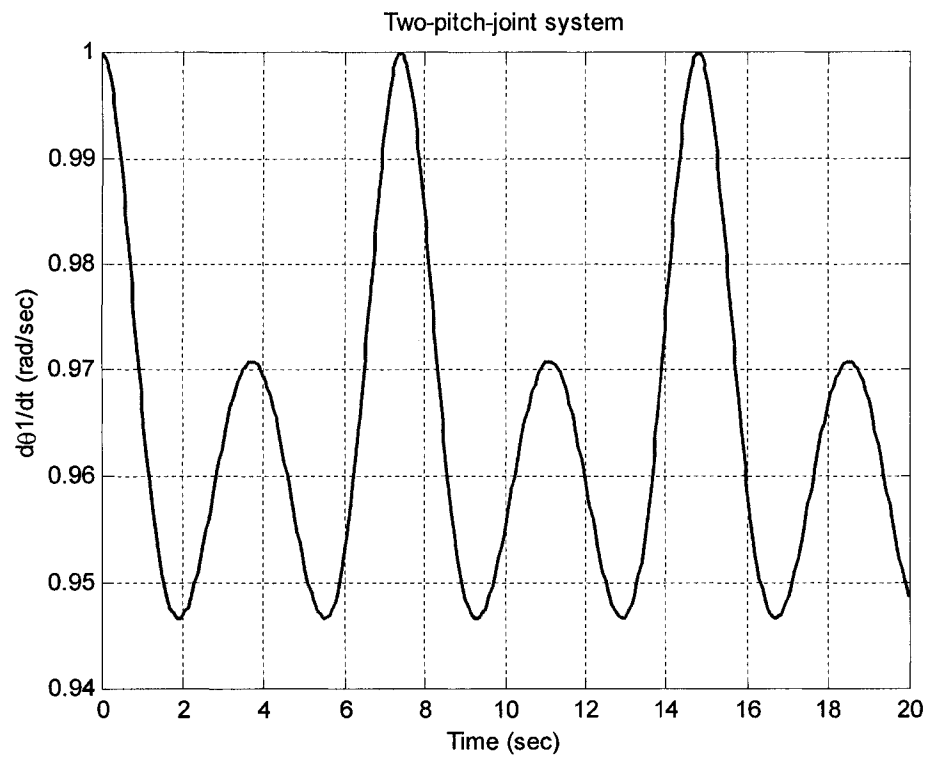


Figure 3.13 1st joint angular velocity versus time at the initial condition:
 $\tau_1 = 0, \tau_2 = 0, \underline{z}_0 = [0 \ 1 \ 0 \ -1]'$

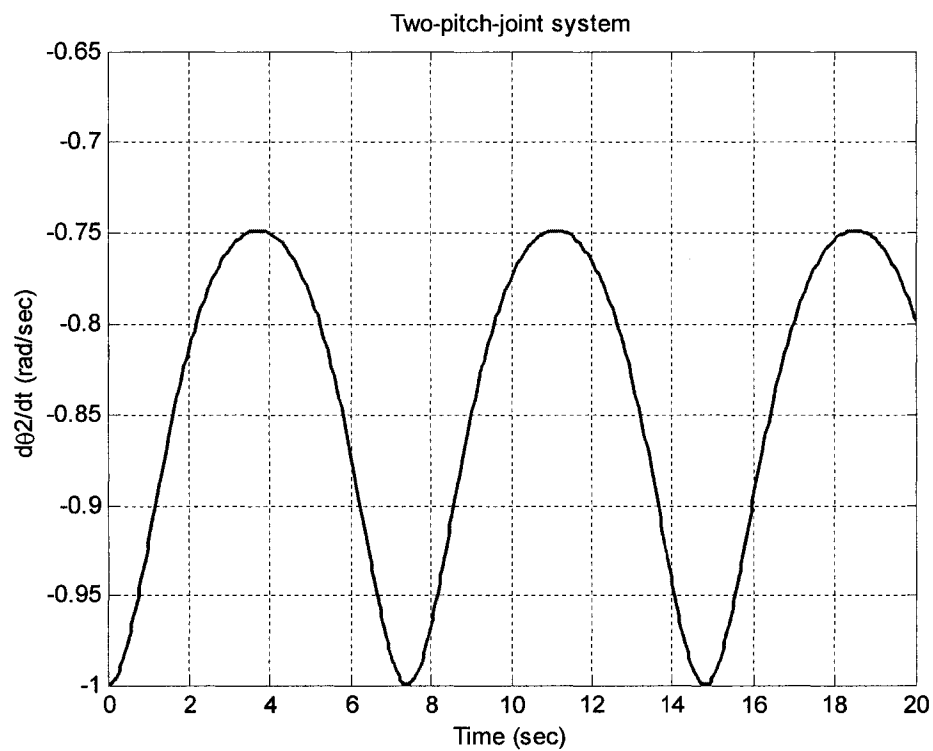


Figure 3.14 2nd joint angular velocity versus time at the initial condition:
 $\tau_1 = 0, \tau_2 = 0, \underline{z}_0 = [0 \ 1 \ 0 \ -1]'$

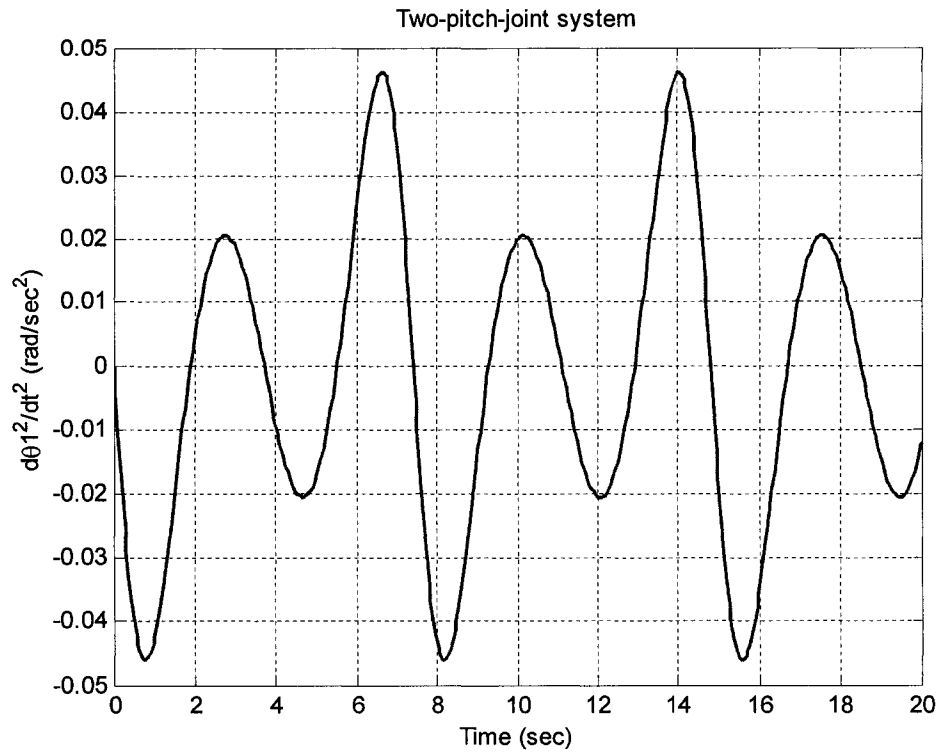


Figure 3.15 1st joint angular acceleration versus time at the initial condition:
 $\tau_1 = 0, \tau_2 = 0, \underline{z}_0 = [0 \ 1 \ 0 \ -1]^T$

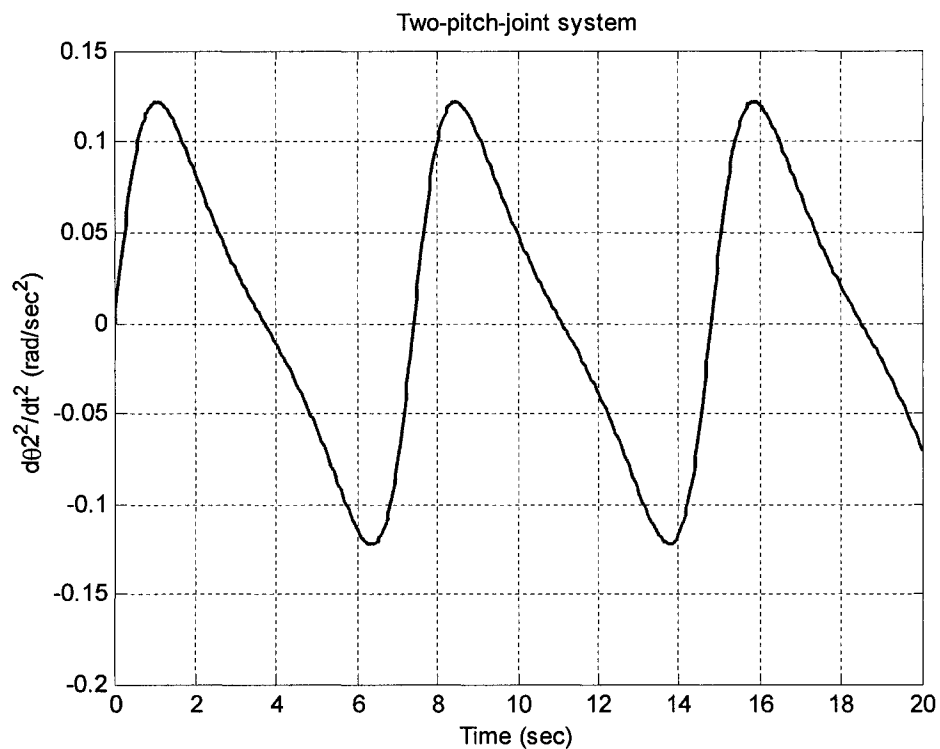


Figure 3.16 2nd joint angular acceleration versus time at the initial condition:
 $\tau_1 = 0, \tau_2 = 0, \underline{z}_0 = [0 \ 1 \ 0 \ -1]^T$

3.3.2 Characteristics in Free Motion in Case of $p = [0 \ 1 \ 0]^T$

In this section, simulate the two-pitch-joint link system using different physical parameters which are listed in Table 3.1 under different initial conditions. We simulate this system according to state space equation (3.34) within Matlab using its ode23 routine. From the results of simulation, we can not find the rule of motion of the two links because of their nonlinear characteristics due to the gravity.

Following is an example of the simulation. Assume point masses $m_1 = m_2 = 1kg$, link lengths $l_1 = l_2 = 1m$. Simulate this two-pitch-joint link system under the following initial condition: $\underline{z}_0 = [0 \ 0.5 \ 0 \ 0.5]^T$ according to state space equation (3.34). Figure 3.17 and Figure 3.18 represent the relationships of 1st and 2nd joint angular displacement versus time respectively.

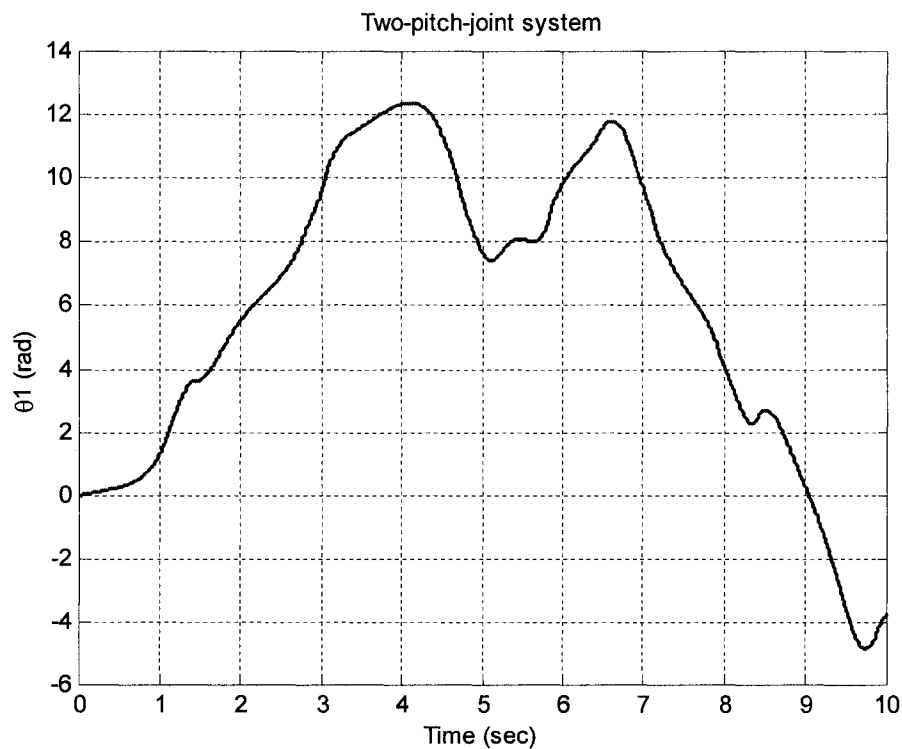


Figure 3.17 1st joint angular displacement versus time at the initial condition:
 $\tau_1 = 0, \tau_2 = 0, \underline{z}_0 = [0 \ 0.5 \ 0 \ 0.5]^T$

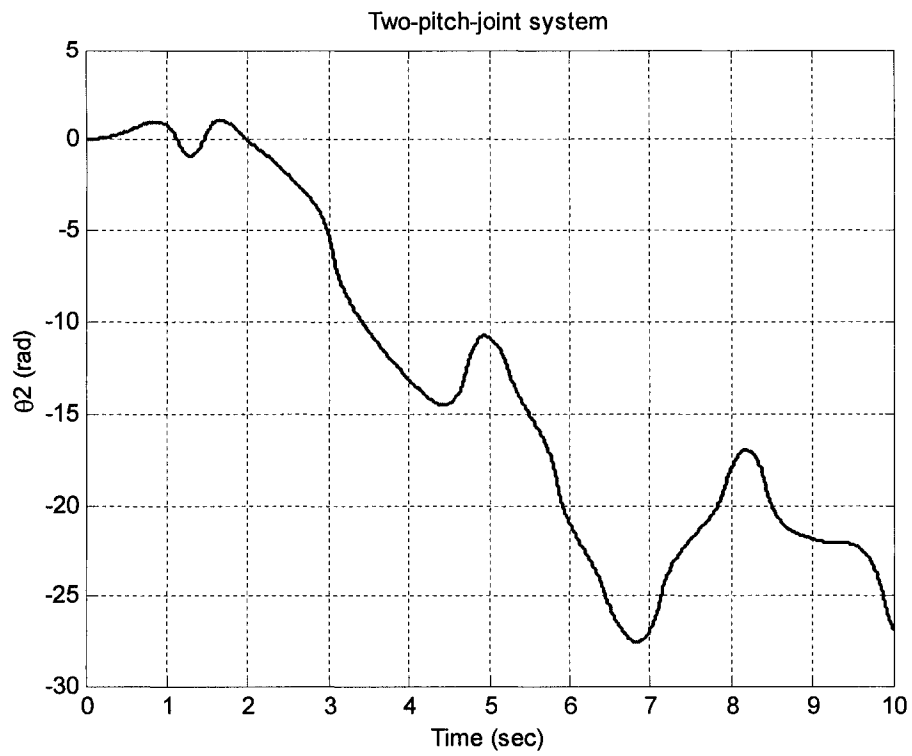


Figure 3.18 2nd joint angular displacement versus time at the initial condition:

$$\tau_1 = 0, \tau_2 = 0, \underline{z}_0 = [0 \quad 0.5 \quad 0 \quad 0.5]^T$$

Figure 3.19 and Figure 3.20 are the plots that represent the relationship of 1st and 2nd joint angular velocities versus time, respectively.

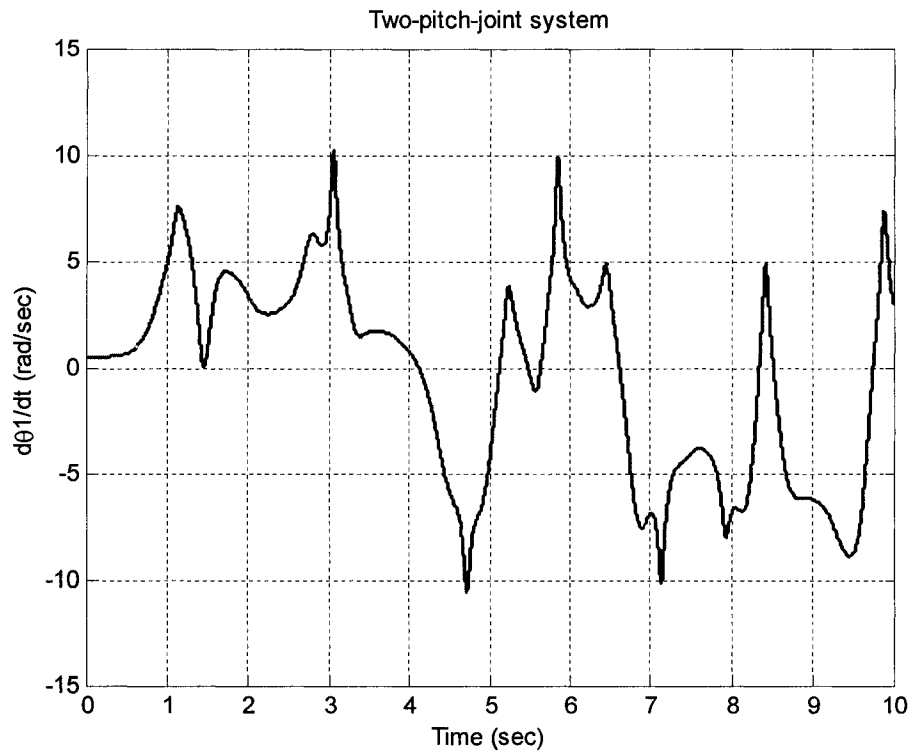


Figure 3.19 1st joint angular velocity versus time at the initial condition:
 $\tau_1 = 0, \tau_2 = 0, \underline{z}_0 = [0 \ 0.5 \ 0 \ 0.5]^T$

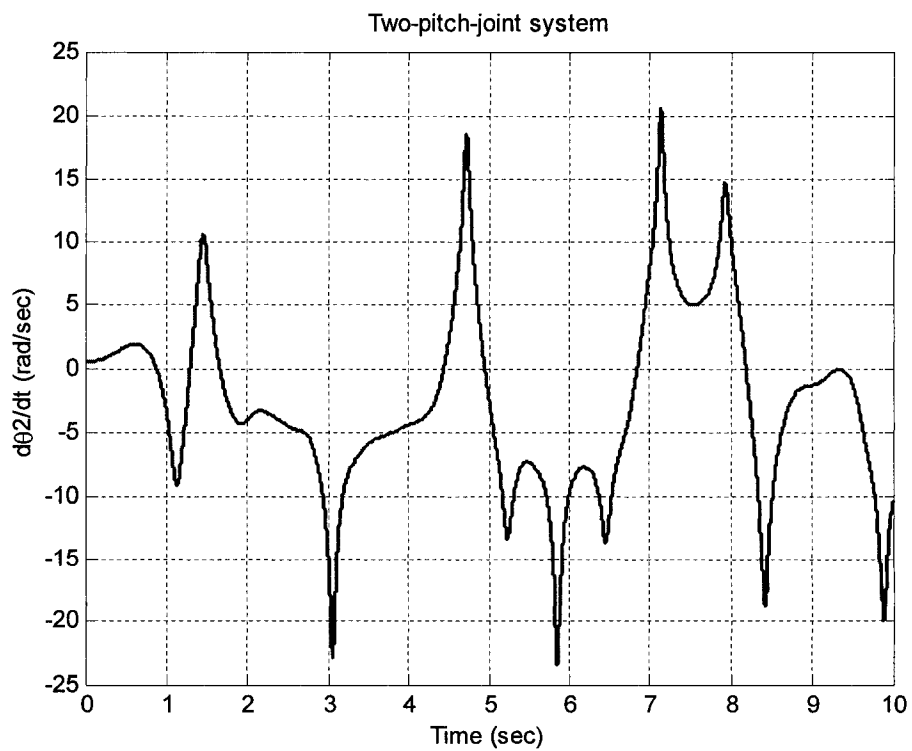


Figure 3.20 2nd joint angular velocity versus time at the initial condition:
 $\tau_1 = 0, \tau_2 = 0, \underline{z}_0 = [0 \ 0.5 \ 0 \ 0.5]^T$

Figure 3.21 and Figure 3.22 are the plots that represent the relationship of 1st and 2nd joint angular accelerations versus time respectively.

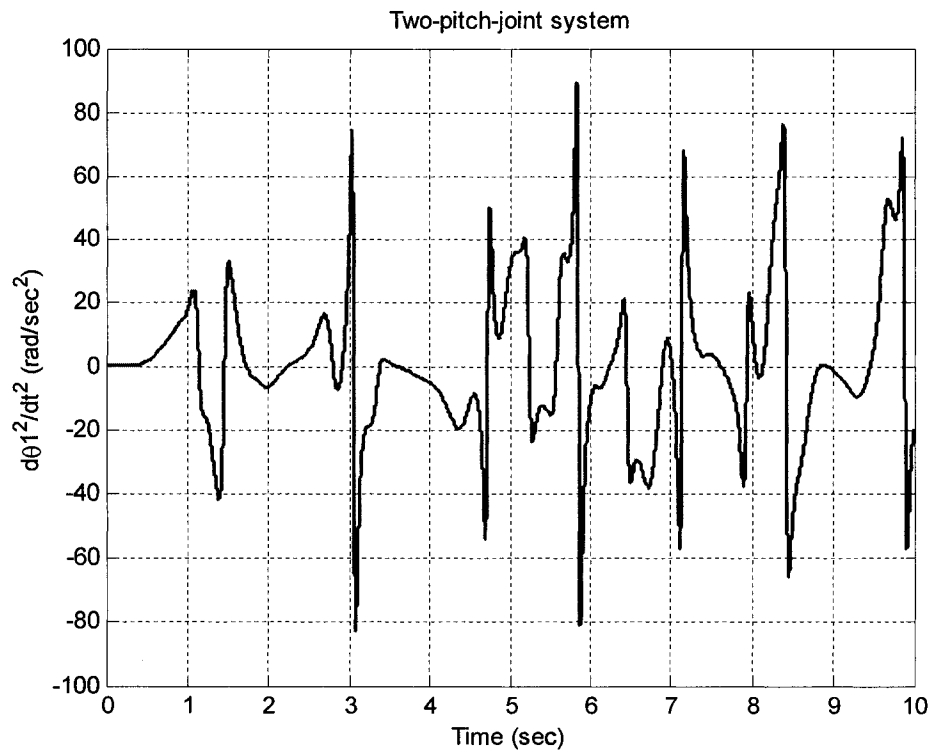


Figure 3.21 1st joint angular acceleration versus time at the initial condition:
 $\tau_1 = 0, \tau_2 = 0, \underline{z}_0 = [0 \ 0.5 \ 0 \ 0.5]'$

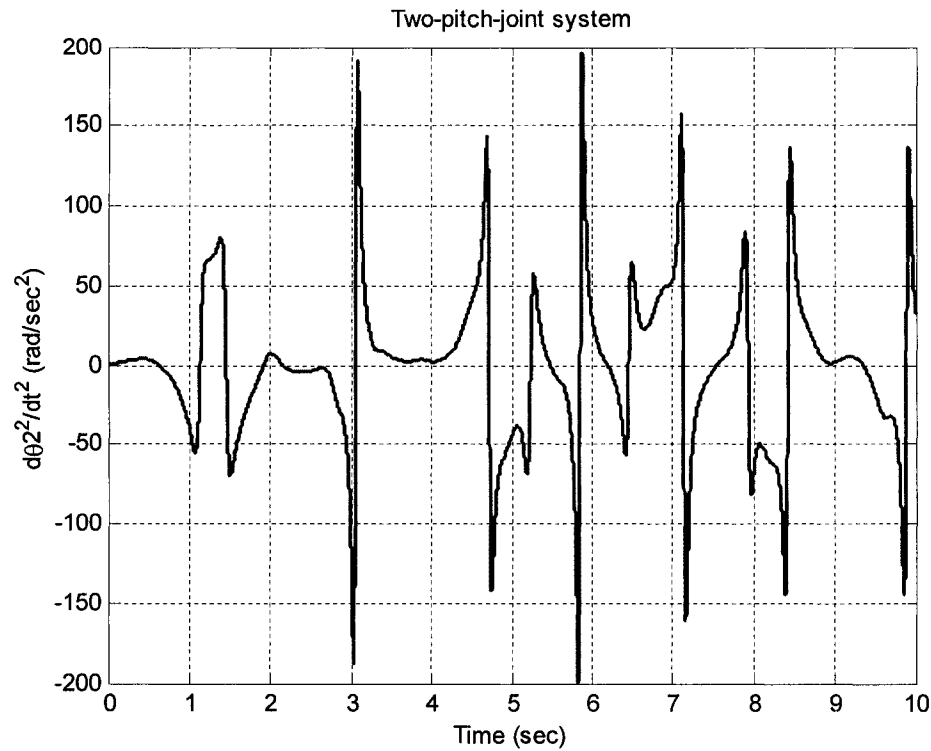


Figure 3.22 2nd joint angular acceleration versus time at the initial condition:
 $\tau_1 = 0, \tau_2 = 0, z_0 = [0 \ 0.5 \ 0 \ 0.5]'$

3.4 Dynamics of Forced Motion

In this section, we will discuss the characteristics in forced motion of the vertical two-

pitch-joint link system. Two cases will be studied. One is in case of $p = \begin{bmatrix} 0 \\ 0 \\ 1 \end{bmatrix}$; and the

other is in case of $p = \begin{bmatrix} 0 \\ 1 \\ 0 \end{bmatrix}$. Assume $m_1 = m_2 = 1\text{kg}$ and $l_1 = l_2 = 1\text{m}$. Let $\lambda = \frac{\tau_1}{\tau_2}$,

τ_1, τ_2 are the actuated torques acting on 1st and 2nd links respectively.

3.4.1 Dynamics of Forced Motion in case of $p = [0 \ 0 \ 1]^T$

Assume $m_1 = m_2 = 1kg$ and $l_1 = l_2 = 1m$. Change $\lambda = 0.1, 1, 5, 10$ respectively, simulate

this system under the initial condition: $\underline{z}_0 = \begin{bmatrix} 0 \\ 1 \\ 0 \\ 1 \end{bmatrix}$. We find:

1) τ_1 is fixed, 1st link keeps rotating. When λ increases, the angular displacement of 1st link keeps unchanged; 2nd link keeps oscillating, when λ increase, the amplitude of the oscillating will decrease.

2) τ_2 is fixed, 1st link keeps rotating. When λ increases, the angular displacement of 1st link increases; 2nd link keeps oscillating, when λ increases, the amplitude of the oscillating will decrease.

Keep the physical parameters unchanged, simulate this system under different initial

condition, for example $\underline{z}_0 = \begin{bmatrix} 0 \\ 0 \\ 0 \\ 0 \end{bmatrix}$. We found that the motion rule of the two links is

different from that of the two links under above initial condition. So the motion rule of the two links is dependent on the initial conditions when the physical parameters are given. The example of plots will not be given here for the purpose of brevity.

3.4.2 Dynamics of Forced Motion in case of $p = [0 \ 1 \ 0]^T$

With point masses $m_1 = m_2 = 1kg$, link lengths $l_1 = l_2 = 1m$. Change $\lambda = 0.1, 1, 5, 10$

respectively, simulate this system under the initial condition: $\underline{z}_0 = \underline{0} = \begin{bmatrix} 0 \\ 0 \\ 0 \\ 0 \end{bmatrix}$. We can

not find the rule of motion of the two links because of their nonlinear characteristics. Figure 3.23 through Figure 3.28 are the example of plots that represent the relationships of joint angular displacement, joint angular velocities and joint angular accelerations versus time respectively when $\tau_1 = \tau_2 = 1Nm$.

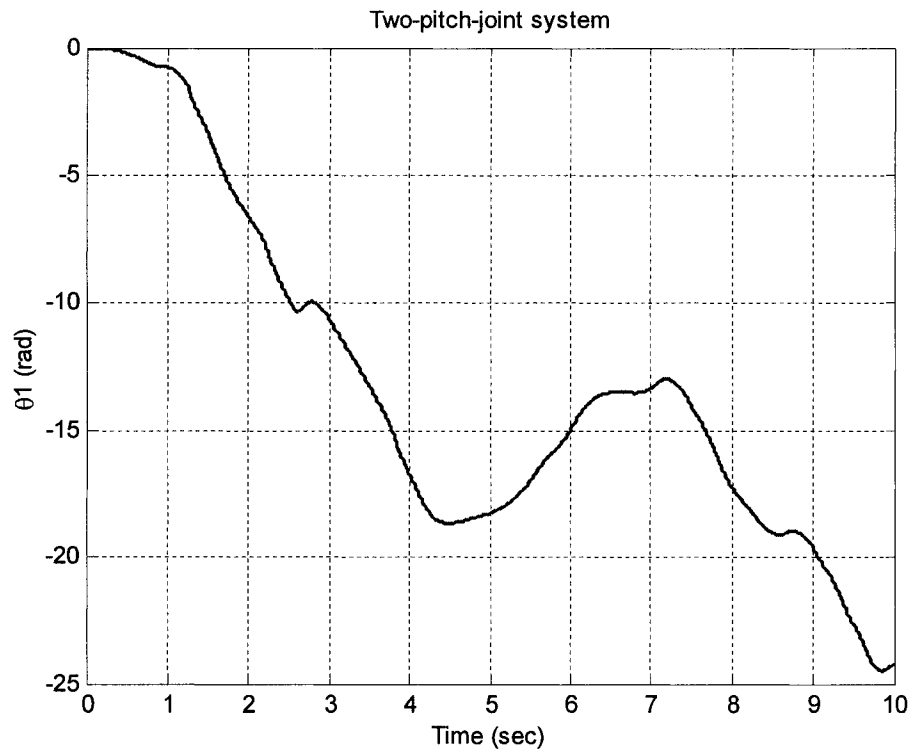


Figure 3.23 1st joint angular displacement versus time at the initial condition:
 $\tau_1 = 1, \tau_2 = 1, \underline{z}_0 = \underline{0}$

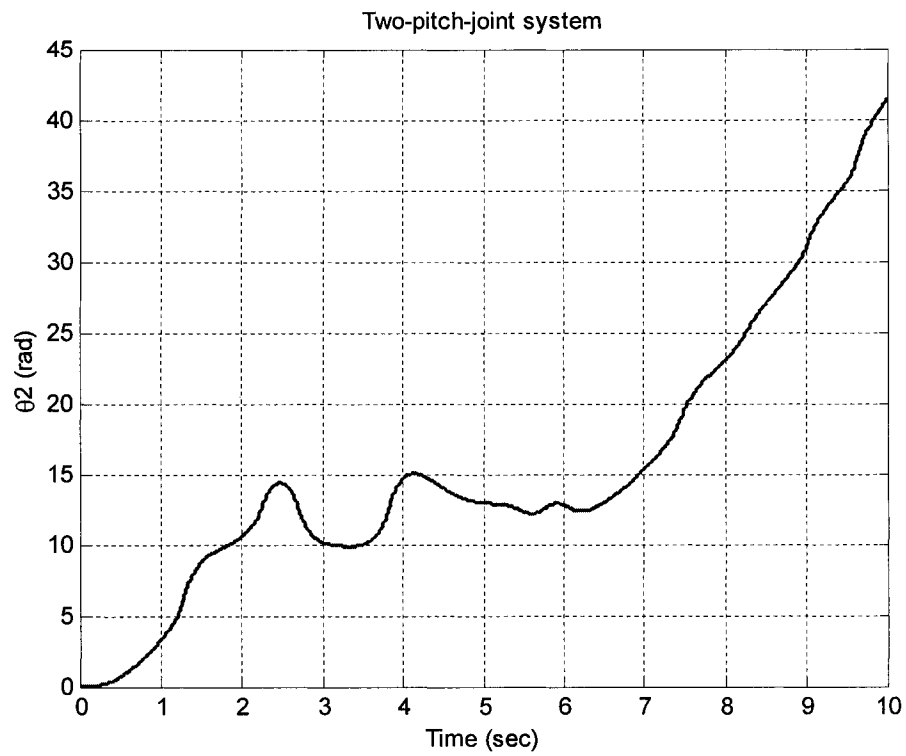


Figure 3.24 2nd joint angular displacement versus time at the initial condition:
 $\tau_1 = 1, \tau_2 = 1, \underline{z}_0 = \underline{0}$



Figure 3.25 1st joint angular velocity versus time at the initial condition:
 $\tau_1 = 1, \tau_2 = 1, \underline{z}_0 = \underline{0}$

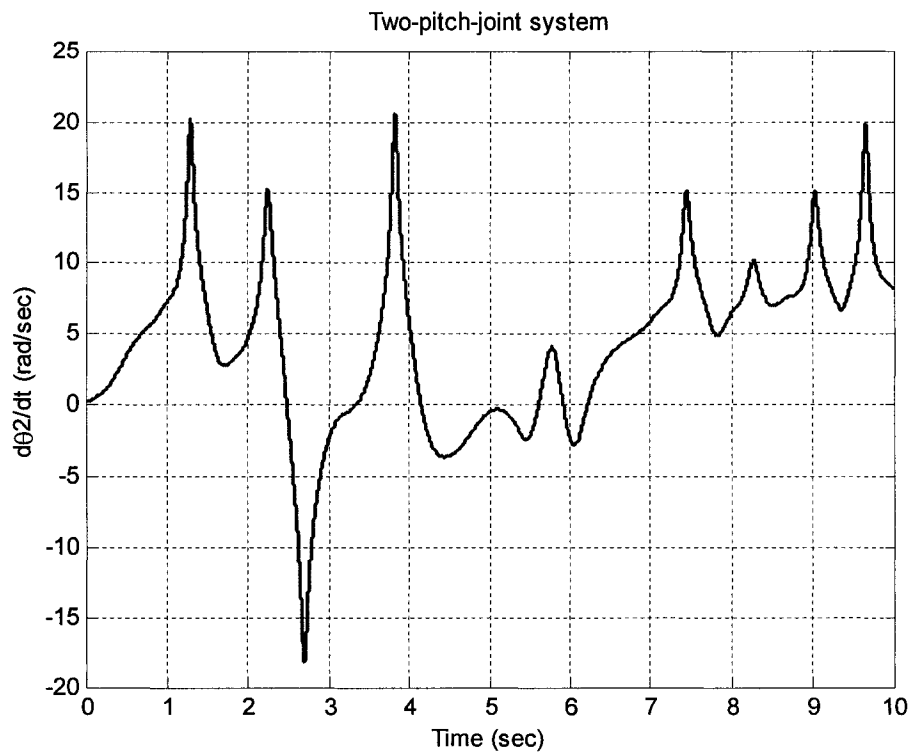


Figure 3.26 2nd joint angular velocity versus time at the initial condition:
 $\tau_1 = 1, \tau_2 = 1, \underline{z}_0 = \underline{0}$

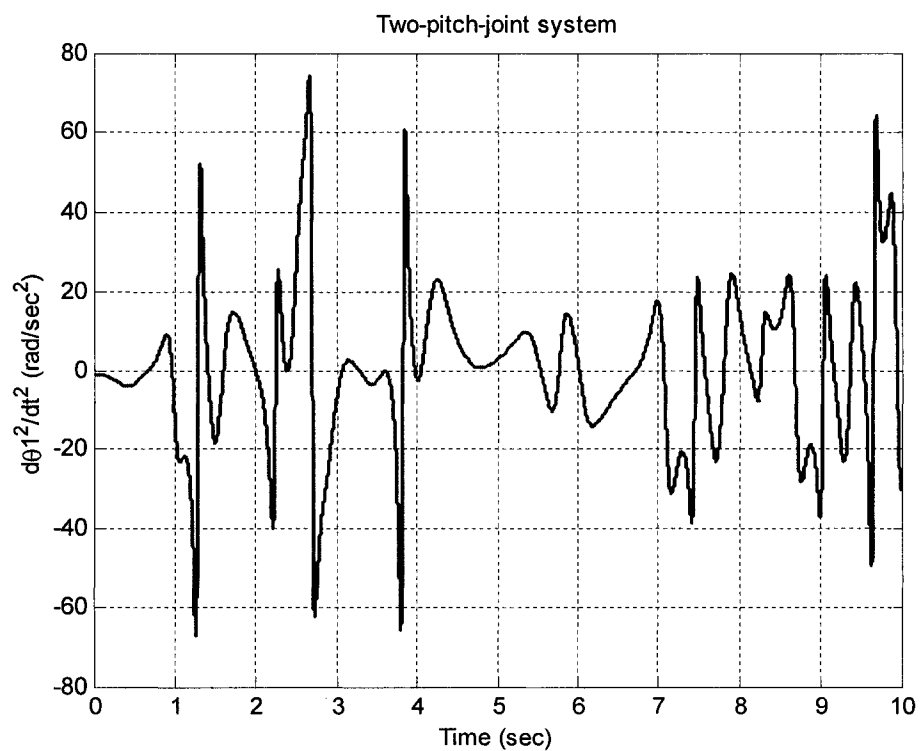


Figure 3.27 1st joint angular acceleration versus time at the initial condition:
 $\tau_1 = 1, \tau_2 = 1, \underline{z}_0 = \underline{0}$

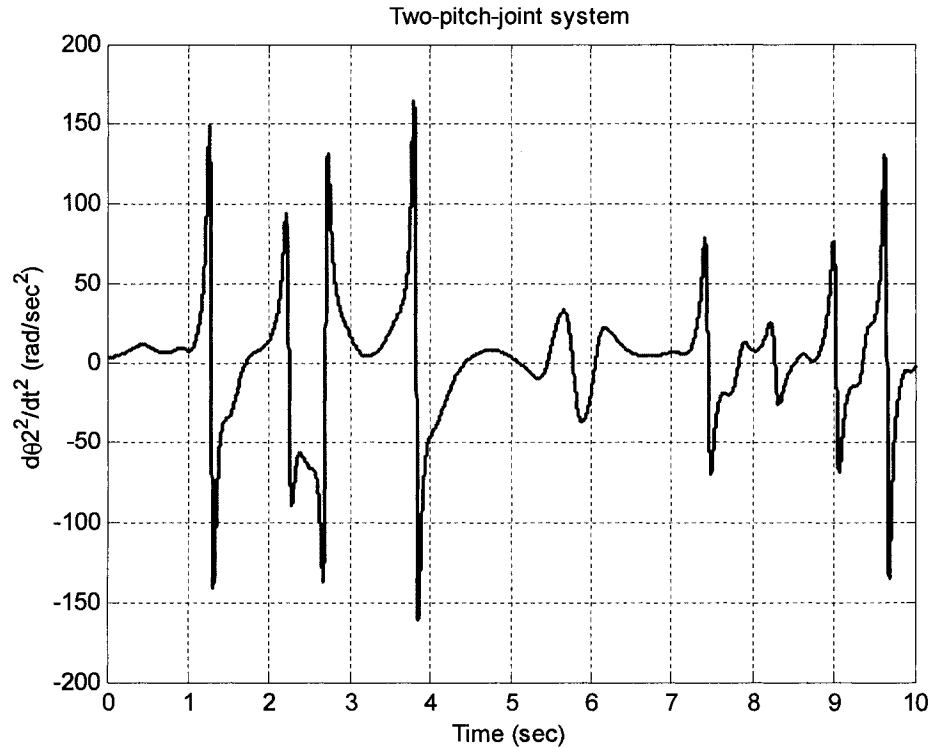


Figure 3.28 2nd joint angular acceleration versus time at the initial condition:
 $\tau_1 = 1, \tau_2 = 1, \underline{z}_0 = \underline{0}$

The plots can be explained by the method of motion analysis and synthesis, but it exceeds the focus of this thesis so it will not be discussed in detail here. Up to now, we have known the dynamics of the forced motion of the two-pitch-joint link system through the results of the simulation. Next, we will give an example which tries to use an appropriate control sequence so as to move the system along the specified path according to its dynamic characteristics. To simplify this problem without losing its generality, we consider the two-pitch-joint link system as a discrete time system. The control input is taken as discrete values and the non-dimensional sampling time is chosen appropriately. The control action is started from the time t_0 , applying a constant torque, and switched by the other value at the time t_1, t_2, \dots, t_n . Also let the interval $t_i \leq t \leq t_{i+1}$ be control interval i , and τ_{2i} is a constant torque at the interval.

Figure 3.29 shows the plots of the relationship between the 2nd joint angular displacement and its angular velocity for the actuated torque at 2nd joint $\tau_{2i}=6, 5$ in the case of $\tau_1 = 3Nm$, $m_1 = m_2 = 1kg$ and $l_1 = l_2 = 1m$ (meter). The plots represent the

forced motion, started from the point O with the initial condition: $\underline{z}_0 = \begin{bmatrix} 0.5 \\ 0 \\ 0.5 \\ 0 \end{bmatrix}$, actuated

by a constant torque, and then switched by another constant torque at the point A, B respectively.

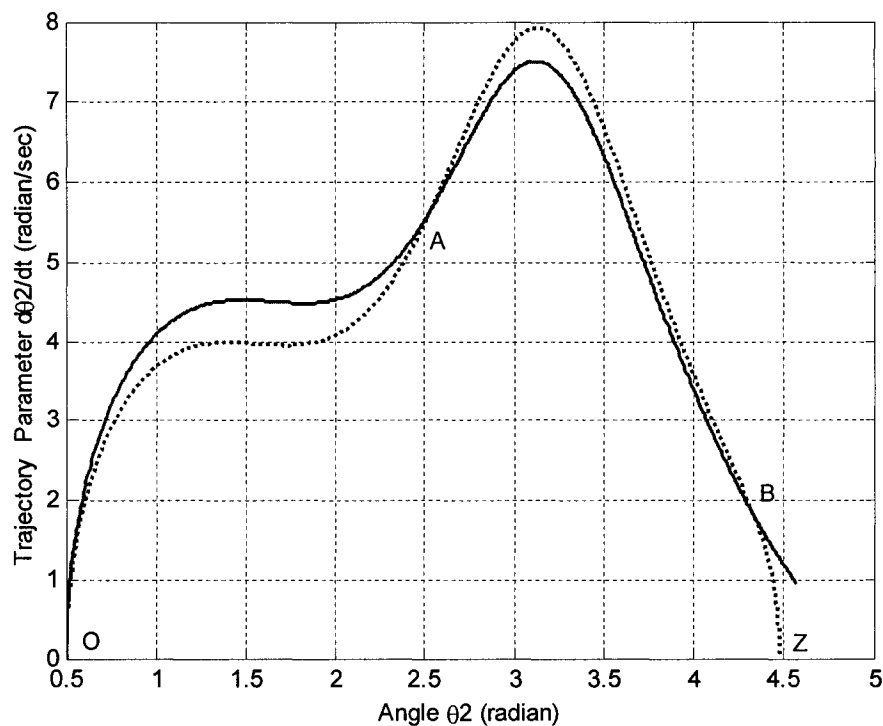


Figure 3.29 The variations of the trajectory parameter $\dot{\theta}_2$ in the case of $m_1 = m_2 = 1kg$ and $l_1 = l_2 = 1m$ (meter), where the solid line is $\tau_{2i}=6$, and the dotted line is $\tau_{2i}=5$.

Here, we show an example of the control action using Figure 3.29. The motion control considered in this example is to move the second link of this system from initial point O to the final point Z, and make the angular velocity of the second joint

equal to zero at the final point Z. At the beginning, the second link is moved from the point O to the point A or B applying $\tau_{20}=6$. At the point A or B, the torque is changed into $\tau_{21}=5$, then the second link moves to the point Z. At the point Z, the angular velocity of the second joint is equal to zero, and then the second link stops applying $\tau_{21}=0$ at this point.

In this example, a simple control action is considered. However, we can discuss the general case switched more times by arbitrary torques. As long as the actuated torque and switched point are given, we can take the motion trajectory schematically by the manner in the above example.

As for the case of the control motion of first link, we can also easily obtain an appropriate control sequence using the same method discussed above. It can be a further study for the motion control of the two link system.

3.5 Conclusion

In this chapter, we modeled the two-pitch-joint link system and derived the motion equations of this system. The motion equations are different when different orientations are chosen. Two orientations are chosen for discussion: one is $\mathbf{p} = [0 \ 0 \ 1]^T$, the other is $\mathbf{p} = [0 \ 1 \ 0]^T$. The characteristics of the free motion mode of this system are discussed. In case of $\mathbf{p} = [0 \ 0 \ 1]^T$, the free motion can be classified into two types according to the different initial conditions. The one is rotation and the other is oscillation. Meanwhile, we know that the angular velocity of this system (or the kinetic energy of this system) determines which motion will appear. Furthermore, from the comparison results, it suggests that solution curves of 2nd joint

angular displacement, angular velocity and angular acceleration can be simplified as corresponding sine waves under certain initial condition.

In addition, we discussed the dynamics of the forced motion of this system for both of the two orientations. Also, we give an example to obtain an appropriate control sequence of the system under the orientation of $p = [0 \ 1 \ 0]^T$. From the example, we know that as long as the actuated torque and switched point are given, we can take the motion trajectory schematically by the manner in the example.

Chapter 4

Conclusions

In this thesis, we have modeled two non-linear dynamical systems mathematically, a one-pitch-joint link system and a two-pitch-joint link system, and derived the motion equations of both systems, then simulated both of the systems numerically using ODE routine such as ode23 with Matlab.

In chapter 2, we modeled a one-pitch-joint link system and drove the motion equations of this system. The equations can be classified into linear and non-linear according to the orientation which is chosen. Characteristics of the free motion and dynamics of the forced motion of this system are discussed. The free motion can be classified into two types. One is rotation and the other is oscillation. Furthermore, it can be shown that the initial conditions determine which motion will appear. Some dynamic characteristics are also shown. The link of this system will keep rotating or oscillating according to the initial conditions. In addition, an example of appropriate control sequence of the system is obtained based on the dynamics of forced motion analysis.

In chapter 3, we modeled the two-pitch-joint link system and derived the motion equations of this system. The motion equations are different when different orientations are chosen. Two orientations are chosen for discussion: one is $\mathbf{p} = [0 \ 0 \ 1]^T$, the other is $\mathbf{p} = [0 \ 1 \ 0]^T$. The characteristics of the free motion

mode of this system are discussed. In case of $\boldsymbol{p} = [0 \ 0 \ 1]$, the free motion can be classified into two types according to the different initial conditions. The one is rotation and the other is oscillation. Furthermore, we know that the angular velocity of this system (or the kinetic energy of this system) determines which motion will appear. In addition, we discussed the dynamics of the forced motion of this system for both of the two orientations. The same as chapter 2, we also give an example to obtain an appropriate control sequence of the system under the orientation of $\boldsymbol{p} = [0 \ 1 \ 0]$.

In chapter 2 and chapter 3, the control consequences of the forced motion of both systems are presented based on the numerical integration approach. As long as the actuated torque and switched point are given, we can take the motion trajectory schematically by the manner discussed in the example of this thesis.

As noted in Chapter 3, the motion equation of a two-pitch-joint link system is still quite complicated, but some progress has been made. However, much work remains to be done to understand the qualitative dynamics of this system.

LITERATURE CITED

1. R.L. Borrelli and C. S. Coleman, *Differential Equation: a modeling perspective*, Chapter 3 section 5, 122-130, 1998.
2. R. L. Woods and K. L. Lawrence, *Modeling and Simulation of Dynamic System*, Chapter 9 section 3, 265-272, 1997.
3. J. R. White, *System Dynamics Lecture Notes*, Chapter 7 section 4, 7.30-7.49, 2002.
4. R. E. Parkin, *Applied Robotic Analysis*, Chapter 9 section 3, 289-294, 1991.
5. C. J. Spiteri, *Robotics technology*, Chapter 2, section 2, 17-19, 1990.
6. R. M. Murray, Z. Li and S. S. Sastry. *A Mathematic Introduction to Robotic Manipulation*. CRC Press, Boca Raton, 1994.
7. C. A. Balafoutis and R. V. Pate, *Dynamic Analysis of Robot Manipulators: A Cartesian Tensor Approach*, KAP Press, 1991.
8. R. J. Schilling and S. L. Harris, *Applied numerical methods for engineers using Matlab and C*, Pacific Grove, CA, 2000.
9. J. Penny and G. Lindfield, *Numerical Methods using Matlab*, Upper Saddle River, NJ: Prentice Hall, 2000.
10. M. W. Decker, A. X. Dang, I. E. Uphoff, "Motion Planning for Active Acceleration Compensation", *Proceeding of 2001 IEEE International Conference on Robotics & Automation*, vol. 2, pp1257-1264.
11. S. X. Yang and M. Meng, "An efficient neural network approach to dynamic robot motion planning", *Neural Networks*, vol. 13, Issue 1, 143-148, 2000
12. N. A. Deshpande and M. M. Gupta, "Inverse kinematic neuro-control of robotic systems", *Engineering Application of Artificial Intelligence*, vol. 11, Issue 1, 55-66, 1998.
13. D. Y. Ieng and M. Chen, "Robot trajectory planning using simulation", *Robotics and Computer-Integrated Manufacturing*, vol. 13, Issue 2, 121-129, 1997.
14. C. Vibet, "Symbolic modeling of robot kinematics and dynamics", *Robotics and Autonomous System*, vol. 14, Issue 4, 301-314, 1995.

15. S. R. Bishop, A. Sofroniou, P. Shi, "Symmetry-breaking in the response of the parametrically excited pendulum model", *Chaos, Solitons and Fractals* 25 (2005) 257-264
16. Kee-Ho Yu, Takayuki Takahashi and Hikaru Inooka, "First integral approach to non-linear motion analysis of a two-link system", *Int. J. Non-linear Mechanics*, Vol. 31, No. 3, 405-412, 1996
17. K. Kowalski and W. H. Steeb, "Symmetries and first integrals for non-linear dynamical system: Hilbert space approach", *I. Prog. Theor. Phys.* 85, 713-722, 1991
18. T. J. Bridges and K. V. Georgiou, "A transverse spinning double pendulum", *Chaos, Solitons and Fractals* 12 (2001) 131-144

BIOGRAPHY

Weitian Liu was born November 16th 1973 in Tianjin, China. He earned his Bachelor of Engineering degree in Mechanical Engineering from National University of Defense Technology in 1996 and Master of Engineering degree in Mechanical Engineering from University of Massachusetts at Lowell in 2004. He was a mechanical engineer in Beijing Aerospace Command & Control Center from 1996 to 2001. He has served as a teaching assistant at Mechanical Engineering Department since 2001. He is also the secretary of Chinese Students and Scholars Association.